

# **The Potential Application of Modified Spruce-based Activated Carbon for Adsorption Chillers**

**Deogratias Uwizeyimana**

Thesis to obtain the Master of Science Degree in  
**Energy Engineering and Management**

Supervisors: Dr. Karol Sztekler  
Prof. Moisés Luzia Gonçalves Pinto

## **Examination Committee**

Chairperson: Prof. Francisco Manuel da Silva Lemos

Supervisor: Dr. Karol Sztekler

Member of the Committee: Prof. Henrique Aníbal Santos de Matos

**June 2021**

## **Acknowledgements**

This thesis work was carried out as part of master program in Energy Transition by Innoenergy Master School. The completion of this program by the author was financially made possible by Innoenergy and for that I am grateful.

I would like to thank my thesis supervisors, Dr. Karol Sztekler and Prof. Moisés Luzia Gonçalves Pinto for their invaluable support and guidance throughout the work process which in different ways contributed to the successful completion of this thesis. I would also like to thank MSc. Wojciech Kalawa for the assistance he provided me in setting up the DVS apparatus for sorption analysis.

Also, special thanks to my parents and siblings for their invaluable moral support and prayers throughout the whole process. To my friends, Tarikul, Temiloluwa, Sambo and Oscar among many, thank you for your encouragement and assistance in my work; your support is gratefully acknowledged.

## **Abstract**

In effort to contribute to the ongoing research of green alternative cooling solutions, this research work studied the adsorption performance of spruce based activated carbon - WA TONG on methanol and the potentiality of this adsorbent pair to be adopted and applied in adsorption chillers. With focus on the low thermal energy powered chillers, the analysis was carried out in sub atmospheric conditions at four adsorption temperature points of 30, 40, 50 and 60 °C. Under the same conditions, WA TONG sample performance was tested against the two commercially available samples CWZ22 and CWZ22P and also a comparative evaluation with the high performing activated carbon methanol pairs available in literature was made. Methanol adsorption uptake for WA TONG sample was found to be as high as 60% of adsorbent weight at adsorption temperature of 30 °C and relative pressure of 1.

Keywords: activated carbon, adsorbents, adsorption chillers, cooling

## **Resumo**

Com o intuito de contribuir para a investigação de soluções alternativas de arrefecimento, este trabalho estuda o desempenho de adsorção do carvão ativado produzido a partir de abeto - WA TONG em metanol e o potencial deste par adsorvente ser adotado e aplicado em chillers por adsorção. Com foco nos chillers de baixa energia térmica, a análise foi realizada em condições subatmosféricas em quatro níveis de temperatura de adsorção de 30, 40, 50 e 60 ° C. Sob as mesmas condições, o desempenho da amostra WA TONG foi testado em comparação com as duas amostras comercialmente disponíveis CWZ22 e CWZ22P e também foi feita uma avaliação comparativa com os pares de metanol de carvão ativado de alto desempenho disponíveis na literatura. A absorção de adsorção de metanol para a amostra WA TONG foi de 60 % do peso de adsorvente à temperatura de adsorção de 30 ° C e pressão relativa de 1.

Palavras-chave: carvão ativado, adsorventes, chillers de adsorção, arrefecimento

## Index

Acknowledgements .....	ii
Abstract.....	iii
Index .....	iv
List of figures .....	vi
List of tables .....	vii
List of Abbreviations .....	viii
1. INTRODUCTION .....	1
1.1. Global energy consumption by sector.....	1
1.2. Current and future trends of space cooling demand.....	2
1.3. Impact of space cooling on climate change .....	3
1.4. Space cooling technologies .....	4
1.4.1. Passive cooling .....	4
1.4.2. Active cooling.....	5
1.5. Objective .....	8
2. ADSORPTION TECHNOLOGY .....	9
2.1. Overview of adsorption phenomenon .....	9
2.2. Adsorption refrigeration cycle.....	9
2.3. Adsorption working pairs.....	11
2.3.1. Physical adsorbents working pair .....	12
2.3.2. Chemical adsorbents working pair .....	13
2.3.3. Composite adsorbents working pair .....	14
2.3.4. Metal organic frameworks (MOFs) .....	14
2.4. Adsorption equilibrium.....	14
2.4.3. Types of adsorption isotherms.....	16
2.5. Potential advantages and limitation challenges facing the use of adsorption chillers .....	17
3. A REVIEW OF ACTIVATED CARBON: USE AND PRODUCTION.....	18
3.1. Properties of activated carbon .....	18
3.2. General production process of activated carbon .....	20
3.2.1. Physical activation of activated carbon.....	21
3.2.2. Chemical activation of activated carbon .....	21
4. EXPERIMENTAL METHODS AND PROCEDURE .....	23
4.1. Preparation and treatment of studied activated carbon samples .....	23
4.2. Choice of adsorbate for the activated carbon system.....	24
4.3. Characterization of the samples .....	25
4.3.1. Porosity, Pore volume, True and Apparent density of the samples .....	25
4.3.2. X-Ray Diffraction analysis.....	26
4.4. Experimental setup of the sorption performance analyzer .....	27
5. RESULTS AND DISCUSSION .....	29
5.1. Adsorption performance analysis results .....	29

5.1.1. Synthesized spruce-based sample – WA TONG .....	29
5.1.2. Commercial samples – CWZ22P and CWZ22 .....	32
5.2. Overall performance takeaways and comparison with in literature activated carbons .....	36
6. CONCLUSION.....	38
Bibliography .....	39

## List of figures

Figure 1 – Energy consumption by sector [3].....	1
Figure 2 – Residential energy consumption by end use in IEA countries, 2017 [5].....	2
Figure 3 – World energy use for space cooling projection [1].....	2
Figure 4 – World primary direct energy consumption by source [2].....	3
Figure 5 – Schematic representation of VCRS system [6].....	5
Figure 6 – Absorption cooling cycle [6] .....	7
Figure 7 – Basic adsorption refrigeration system. A. Heating and pressurization. B. Desorption and condensation. C. Cooling and depressurization. D. Adsorption and evaporation [25].....	10
Figure 8 – Adsorption isotherm .....	15
Figure 9 – A typical adsorption isobar .....	15
Figure 10 – Classification of adsorption isotherms according to IUPAC.....	16
Figure 11 - Pore structure network of activated carbon [15] .....	18
Figure 12 – Surface groups commonly found in activated carbons [15].....	20
Figure 13 – General industrial flow chart for the production of thermal activated carbons [15].....	21
Figure 14 – XRD pattern of CWZ22 sample.....	26
Figure 15 – XRD pattern of CWZ22P sample .....	26
Figure 16 – XRD pattern of WA TONG sample.....	27
Figure 17 – DVS Vacuum gravimetric sorption analyzer [38] .....	28
Figure 18 – Methanol adsorption on WA TONG at 30 °C. a) isotherm, b) kinetics.....	29
Figure 19 – Methanol adsorption on WA TONG at 40 °C. a) isotherm, b) kinetics.....	29
Figure 20 – Methanol adsorption on WA TONG at 50 °C. a) isotherm, b) kinetics.....	30
Figure 21 – Methanol adsorption on WA TONG at 60 °C. a) isotherm, b) kinetics.....	30
Figure 22 – An illustrative stack depiction of WA TONG sample adsorption isotherms at different temperatures .....	31
Figure 23 – Methanol adsorption on CWZ22P at 30 °C. a) isotherm, b) kinetics .....	32
Figure 24 – Methanol adsorption on CWZ22P at 40 °C. a) isotherm, b) kinetics .....	32
Figure 25 – Methanol adsorption on CWZ22P at 50 °C. a) isotherm, b) kinetics .....	33
Figure 26 – Methanol adsorption on CWZ22P at 60 °C. a) isotherm, b) kinetics .....	33
Figure 27 – An illustrative stack depiction of CWZ22P sample adsorption isotherms at different temperatures .....	34
Figure 28 – Methanol adsorption on CWZ22 at 30 °C. a) isotherm, b) kinetics.....	34
Figure 29 – Methanol adsorption on CWZ22 at 40 °C. a) isotherm, b) kinetics.....	35
Figure 30 – Methanol adsorption on CWZ22 at 50 °C. a) isotherm, b) kinetics.....	35
Figure 31 – Methanol adsorption on CWZ22 at 60 °C. a) isotherm, b) kinetics.....	35
Figure 32 – An illustrative stack depiction of CWZ22 sample adsorption isotherms at different temperatures .....	36

## List of tables

Table 1 – Lifetime, ODP and GWP of refrigerants [8] .....	4
Table 2 – Sample density, porosity, and pore volume analysis results .....	25

## **List of Abbreviations**

GDP – Gross Domestic Product

EIA – U.S. Energy Information Administration

OECD – Organization for Economic Co-operation and Development

ACs – Air Conditioning Systems

VCRS - Vapour Compression Refrigeration System

CFCs – Chlorofluorocarbons

HFCs – Hydrofluorocarbons

HCFCs – Hydrochlorofluorocarbons

ODP – Ozone Depleting Potential

GWP – Global Warming Potential

COP – Coefficient of Performance

MOFs – Metal Organic Frameworks

IUPAC – International Union of Pure and Applied Chemistry

BET – Brunauer–Emmett–Teller

CFBL – CleanFlow Black Lignin

SCP – Specific Cooling Power

XRD – X-Ray Diffraction

DVS Vacuum – Dynamic Vapor Sorption Vacuum



# 1. INTRODUCTION

In recent years, most parts of the world have been experiencing very hot summers and some of the harshest heat waves to date. The annual global temperature keeps rising. Since 1981, the global annual temperature has been increasing at an average rate of +0.18 °C per decade [33]. In the light of climate change threat and ever-increasing unpredictability of weather conditions across the globe, humans are looking for ways to mitigate the effects of this new reality on their well-being and overall economic productivity. The prominent problem people are facing is heat discomfort due to high temperatures. On a local scale, since their inception, the electric air-cooling systems have been the go-to solution in dealing with this challenge. However, the poor efficiency of these systems leads to high power consumption which in the grand-scheme of energy cycle happens to be counterproductive towards the mission of reducing global emissions. As of 2018, the use of air conditioners and electric cooling appliances accounted for 20% of the total electricity consumption in buildings worldwide [1]. As the world's emerging economies mainly in tropical hot areas, keeps growing along with their demographic growth, the global cooling demand is expected to rise. As income and standards of living improve, people will naturally want to ensure thermal comfort in their homes regardless of the ambient state. This will impose a significant strain on local electricity grids as the overall energy demand increases and it will in turn drive up the conventional firing emissions as long as the renewable alternatives aren't self-sufficient yet.

## 1.1. Global energy consumption by sector

Global energy consumption refers to the sum total amount of energy used by individual consumers worldwide. The rate of consumption is typically dictated by the two main factors: regional climate and country income level. It is widely believed that the economic growth and energy consumption goes together. However, this relationship is not unidirectional, in case of developing countries, access to electricity tends to stimulate the growth of Gross Domestic Product (GDP) to a certain extent, while in developed countries, the higher the country's GDP the higher total energy consumption.

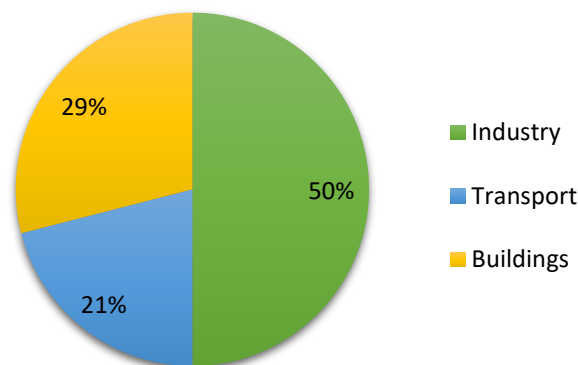


Figure 1 – Energy consumption by sector [3]

In all sectors, the energy demand trend keeps rising. As of 2019, the industrial sector accounts for around half the global energy consumption, transport 21% and with commercial and residential buildings about 29% [3]. The U.S. Energy Information Administration (EIA) projects that global energy

consumption in buildings will grow by 1.3% per year on average from 2018 to 2050. In countries that are not part of the Organization for Economic Cooperation and Development (non-OECD countries), EIA projects that energy consumed in buildings will grow by more than 2% per year [4]. Residential electricity consumption comes mainly in form of lighting, appliances, space and cooling.

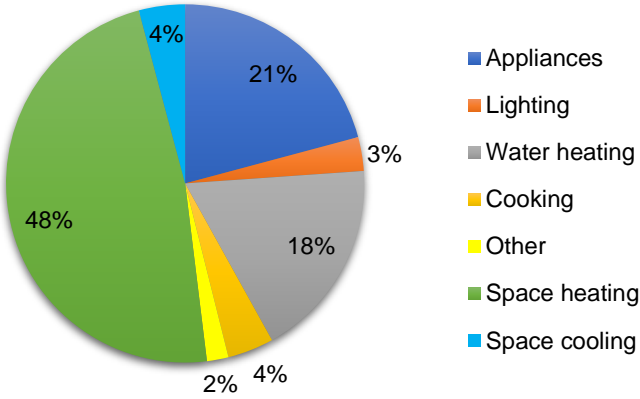


Figure 2 – Residential energy consumption by end use in IEA countries, 2017 [5]

**1.2. Current and future trends of space cooling demand**

Energy demand for space cooling is fundamentally defined by the efficiency of adopted cooling systems and the accessibility of those systems to masses. In hot and humid parts of the world, the continual rising of income will lead to more ownership of air conditioning systems (ACs) at both household and commercial building scale. Currently, the average efficiency of ACs is more or less the same for both commercial and household scale units. However, in the coming future, it is projected that the efficiency will remarkably improve for large scale ACs. This reflects the fact that commercial ACs grow in size, partly due to new commercial installations shifting to chillers that cool the whole building, offering greater opportunity for adopting more efficient technologies i.e., the efficiency tends to increase with size.

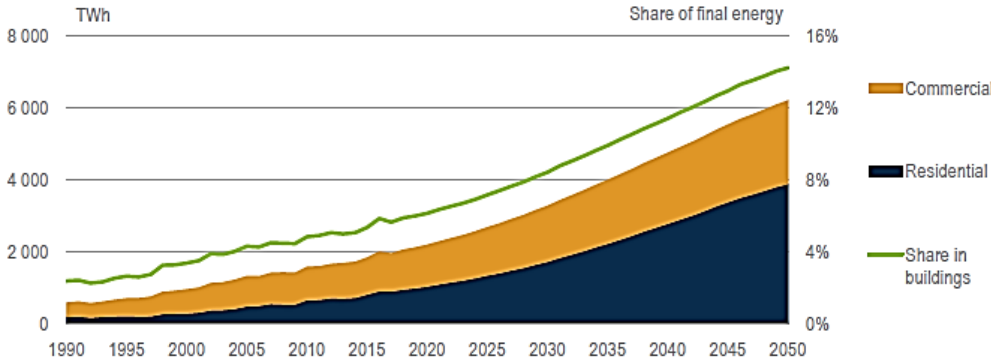


Figure 3 – World energy use for space cooling projection [1]

Though it is projected that the ACs efficiencies are to increase considerably in the future, the increasing degree of ownership of ACs worldwide is expected to offset the effect the improved efficiency. From 2016 to 2050, the energy consumption for space cooling is expected to rise from 2020 terawatt hours

(TWh) to 6200 TWh. This almost threefold increase in demand is mainly from residential sector which will account for about 70% of the jump by 20250 [1].

In general, global electricity use in buildings and other sectors grows with time. However, there's no end use projected to grow as fast as space cooling. Eventually, this will make cooling the largest user of electricity in buildings ahead the rest of end-uses. Most of the projected growth in energy use for space cooling is set to come mainly from India, China and other developing countries.

**1.3. Impact of space cooling on climate change**

As cooling demand increases, its strain on electric power grid will continue to rise. The rising of cooling's share in electricity demand which is still generated mainly from conventional fossil fuels will inevitably lead to the more carbon emissions. As of 2019, conventional cooling installations and appliances accounted for about 10% of all global greenhouse gas emissions which at the time was more than twice the emissions from aviation and maritime vessels combined [7]. The projections indicate that if the currently in use cooling systems and their governing policies are left unchecked, the emissions from cooling are expected to double by 2030 and triple by 2100 as a result of urbanization, population growth and anticipated heatwaves [7]. There's a potential causal nexus, as the earth's temperature keeps rising, increased demand for cooling will drive up levels of emissions which in turn will led to higher temperatures and therefore make the need for access to cooling even more critical and this poses a dangerous threat to life on earth in general.

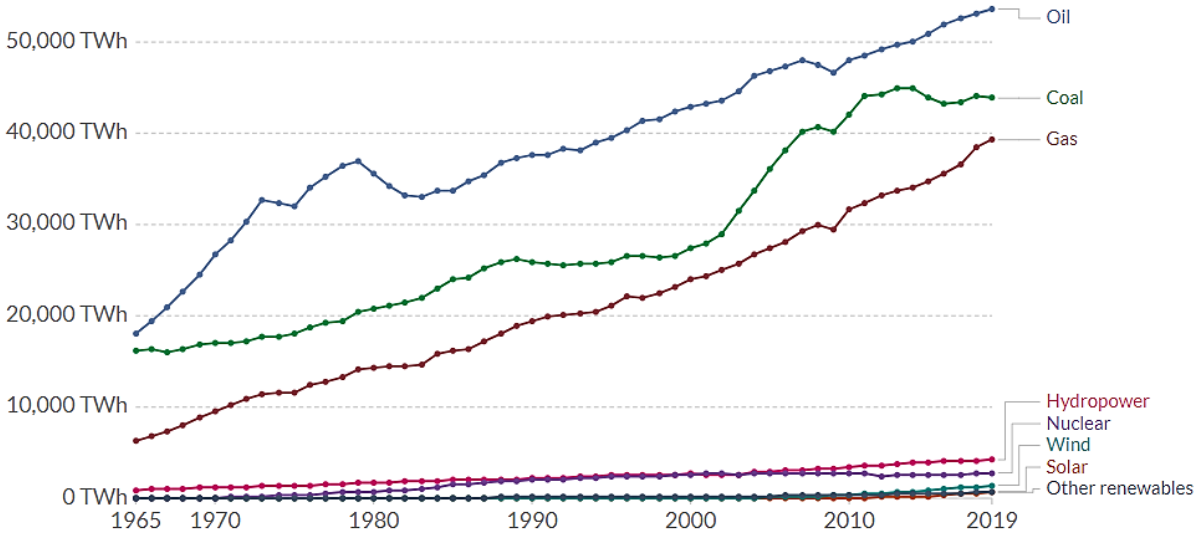


Figure 4 – World primary direct energy consumption by source [2]

Figure 4 shows the amount of energy consumed by source in its raw form meaning not accounting for the inefficiencies of conversion technologies. This substantiate the likeliness of increase in conventional fossil fuel burning i.e., more emissions whenever there's an extra strain imposed to power grid since these are currently the prominent energy resources available.

A large proportion of the cooling market is dominated by vapour compression refrigeration system (VCRS) solutions that rely heavily on use of refrigerants like chlorofluorocarbons (CFCs), hydrofluorocarbons (HFCs) and hydrochlorofluorocarbons (HCFCs) which are one of the main agents

of ozone layer depletion. Due to in time leakage that exists within these VCRS, the refrigerants come into contact with the atmosphere and reacts with ozone layer which results into ozone depletion. Leakage leads to an unwanted refrigerants production cycle to compensate for lost amounts of refrigerants, on estimate only 35% of total refrigerants produced is for the new air conditioners and refrigerants, the rest 65% comes for refill purposes [8].

Using the indexes of ozone depleting potential (ODP) and global warming potential (GWP), the impact of these refrigerants is depicted in table 1 below.

Table 1 – Lifetime, ODP and GWP of refrigerants [8]

Refrigerant	Life cycle (Years)	ODP	GWP (100 years)
Halons	20 to 70	3 to 10	1300 to 18000
CFC-11	45	1	3800
CFC-12	100	1	8100
CFC-115	1700	0.6	9300
HCFC	1 to 20	0.05	400 to 1800
HFC	1 to 300	0	140 to 11700
Ammonia (NH <sub>3</sub> )	Few days	0	0

\* ODP is the index that shows the impact of coolant on ozone depletion and is calculated based on R11 or R12 whose ODP is assumed to be one. While GWP is the index to determine the greenhouse effect of a coolant and is calculated based on CO<sub>2</sub>, whose GWP is equal to one [8].

## 1.4. Space cooling technologies

According to the laws of thermodynamics, for two non-isolated systems with different temperatures, the energy in form of heat is transferred from a hot body to a cold body until the equilibrium between two systems is reached. To achieve the cooling effect goes against this natural law and therefore for the energy to be transferred from a cold temperature to a hot temperature system, the external work has to be applied onto the system. That external work is performed by a cooling system.

The effective management of space thermal comfort in a building is fundamentally based on its architectural design. There exists so many cooling techniques and the choice of a proper technique to be deployed in a building is a crucial step in an attempt to attain the highest possible efficiency and proper energy use. The cooling technologies are divided into two broad categories: active and passive cooling techniques.

### 1.4.1. Passive cooling

Passive cooling is a technological design for providing cooling to the buildings by using the minimum possible amount of electrical energy. Passive cooling often runs on renewable energy sources. Passive cooling attains high levels of natural convection and heat dissipation by utilizing a heat sink material to maximize the radiation and convection heat transfer modes. Natural resources like wind or soil are used as heat sinks to absorb or dissipate heat. This leads to proper cooling ensuring thermal comfort in homes or office buildings by keeping them at the desired temperatures.

This technique should preferably be the default choice for space cooling considering its low financial cost. However, given the high cooling demand most buildings require, it is important to pair passive with active cooling system. Different types of passive cooling methods are derived based on the internal gain of heat, transfer of heat in an envelope form along with transfer of heat occurring in outdoor and indoor air mixed of them. These techniques are currently deployed in most new ecofriendly passive houses. Passive cooling techniques include: *night ventilation, radiant cooling, ground cooling and evaporative cooling techniques.*

**1.4.2. Active cooling**

Active cooling refers to cooling techniques that rely on an external system to enhance heat transfer within a space. Through active cooling technologies, the rate of fluid flow increases during convection, which dramatically increases the rate of heat removal. Active cooling systems rely predominantly on electrical energy as the main process driver. Active cooling technologies include: *mechanical vapour compression system, absorption, desiccant and adsorption cooling systems.*

**i. Mechanical vapour compression system**

VCRS is a cooling system that uses liquid refrigerant in a closed cycle which circulates the refrigerant through four stages in which it undergoes compression and expansion phases, changing it from liquid to vapor. The cooling effect is achieved due to heat being either absorbed or released by the system, resulting in a change in temperature of the surrounding air that is passing over the unit's components.

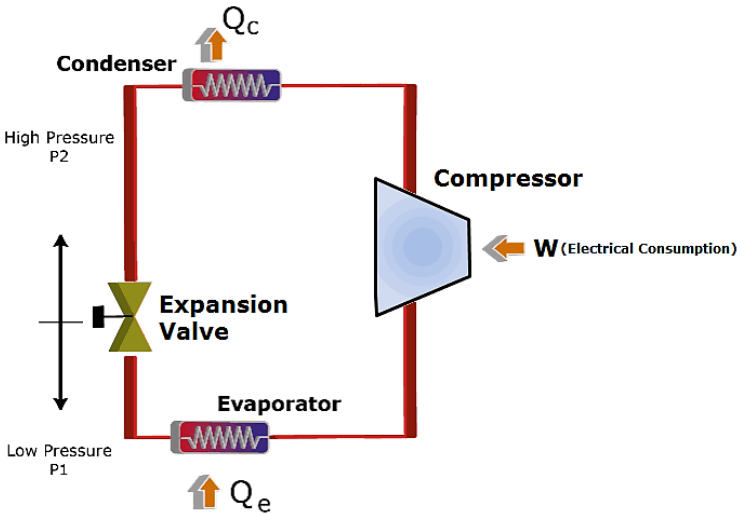


Figure 5 – Schematic representation of VCRS system [6]

The working principle of VCRS is as follows: VCRS system is comprised of four main components: the evaporator, condenser, compressor and expansion valve. At first, the VCRS is filled with a liquid refrigerant. Once the system turns on, the refrigerant passes through the compressor, turning it into a high pressure/high temperature vapor. Then it flows through the condenser coils, designed to allow airflow to the exterior. As ambient air from outside blows across the condenser coils, it carries away the excess heat, allowing the vapor to cool and condense into liquid. From here, the liquid flows to the expansion valve where it is rapidly expanded back into a low-pressure vapor. Due to sudden drop in

pressure, the refrigerant undergoes a drastic drop in temperature. With the cooled refrigerant flowing into the evaporator coils, a fan inside the unit directs air over the supercooled coils and into the targeted space. As the air from the fan passes over the cold coils, it is also cooled, which fills the space with cold air. This also has the effect of warming the refrigerant back up by taking the heat out of the room. As this exchange happens, the refrigerant flows back to the compressor so that it can be sent outside to release the excess heat. The precise space temperature control is achieved through adjustment of the expansion and compression rate [6].

Mechanical vapour compression systems are widely adopted for space cooling in buildings as they have reliable performance and easy controllability. Unitary air-conditioners are popular in residential buildings due to their easy installation and maintenance, while in commercial buildings the centralized water chillers are the preferred option.

## **ii. Absorption cooling system**

Compression chillers are electric power intensive and pose the noise pollution discomfort. Hence, the new trend is to rely more on absorption chillers as an alternative option. Absorption chillers are widely regarded as ideal cooling system in places where power grid is unreliable or costly since they use low grade energy like waste heat to power the process. The low cost of this system explains its application in generating district cooling by using residual heat from power plants and other industrial processes. Overall, the total energy used in the absorption cycle is higher than the energy used in the vapor compression cycle. However, the form of the energy used is not the same: the VCRS cycle uses electricity as input and the absorption cycle uses heat input as the prime driver and some electricity for auxiliary components including like pump.

Absorption cycle is a thermochemical process. The underlying principle of absorption chiller exploits the fact that at certain pressure and temperature certain substances have particular affinity to other substances and this affinity can change when the conditions are altered. In principle absorption chiller and VCRS cycle are the same, the difference comes in how the refrigerant pressure is increased from evaporation to condensation level. In absorption cycle the refrigerant vapor are not compressed but rather are dissolved in an absorbent and the product mixture is transferred to higher pressure zone by a pump [6].

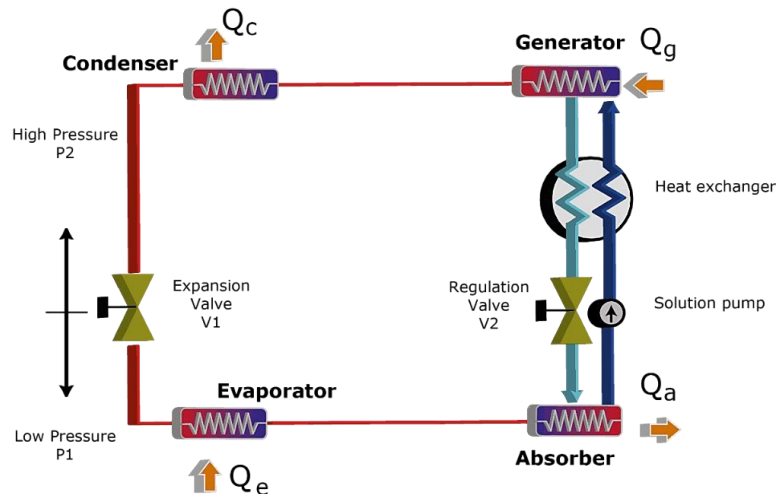


Figure 6 – Absorption cooling cycle [6]

The working principle of an absorption cycle is as follows: the key components of the system are a generator, a condenser, an evaporator and an absorber. In the generator, refrigerant vapor is produced by a heat source from the strong solution. Then the vapor passes through a rectifier for dehydration before entering the condenser. Now the high pressure and dehydrated refrigerant it is condensed. After cooling, the refrigerant passes through an expansion valve where pressure and temperature are reduced to the values below the conditions in the evaporator. Then the cooled refrigerant enters the evaporator and absorbs heat to form saturated vapor. Next the vapor enters the absorber where it is exposed to a spray of a weak refrigerant solution. Which in turn shifts the weak solution to high concentration. The resulting strong solution is then pumped to the generator through a heat exchanger to ensure the solution attains the pressure conditions at the generator level. And the cycle repeats itself. The common working pairs for absorption chillers are Lithium-bromide (LiBr) or Ammonia-water ( $\text{NH}_3\text{-H}_2\text{O}$ ) [6].

### iii. Desiccant cooling system

Desiccant cooling is a thermally driven cooling system widely considered as an alternative to the conventional VCR and absorption cooling systems. It combines the principle of adsorption dehumidification and evaporative cooling. Desiccants can be either solid or liquid substances. In solid desiccant systems, a dry solid desiccant is used in a rotating bed or impregnated into honeycomb-form wheel within the system. Liquid desiccant systems are a new emerging technology consisting of a contact surface, which is either a cooling coil or cooling tower, wetted with liquid desiccant.

The operation of a desiccant cooling system relies on the use of a desiccant wheel to absorb moisture from air. The dry air is at first cooled in a sensible heat exchanger and then further cooled by an evaporative cooler. The resulting cooled air is then redirected to the targeted space/room. The desiccant system can either be an open or a closed system. In open system, the desiccants are in a direct contact with process air during the dehumidification phase while in a closed system, the air dehumidification happens indirectly. For the purpose of regenerating in-use desiccants, a heat supply is required. Usually, low-grade heat at a temperature of about 60–95°C is sufficient for regeneration, so renewable energies

such as solar and geothermal heat as well as waste heat from conventional fossil-fuel systems may be used. The system is simple and thermal coefficient of performance is usually satisfactory.

### **1.5. Objective**

The rise in global cooling demand mainly in residential sector poses a serious potential strain on electrical grid load if a drastic improvement on the current in use cooling systems is not achieved sooner. One of the promising candidate solutions for this issue is the adsorption-based cooling systems namely adsorption chillers. Currently, adsorption cooling solutions are still in the research phase and most proposed prototypes are at a viability market competitiveness disadvantage in comparison to alternative cooling solutions due to technical limitations of adsorption chillers. The core component of an adsorption system is the adsorbent adsorbate pair applied in the system and this is the utmost defining factor on the system performance. For the system to be practically viable, adsorbent must have high sorption performance, good thermo-physical properties, be abundantly available and cheap. Hence, the goal of this thesis is to explore whether a biomass spruce based activated carbon can be the adsorbent to fulfil the above highlighted premise and also to see how such adsorbent fair in comparison to the best activated carbon samples currently available on the market.



## **2. ADSORPTION TECHNOLOGY**

### **2.1. Overview of adsorption phenomenon**

Adsorption refers to the preferential concentration of certain substances on the surface of a solid or a liquid. It is a boundary phenomenon between two phases, in which cohesive forces act between the molecules of all substances irrespective of their state of aggregation. In adsorption cooling terms, it occurs due to interaction between adsorbate molecules and surface of the adsorbent. Adsorption capacity of an adsorbent largely depends on its surface characteristics such as pore volume/size and surface area. Adsorption phenomenon comes into two forms of processes, physical and chemical adsorption. Physical adsorption is a non-selective molecular interaction on the surface of adsorbents driven by the weak electrostatic interactions including London forces, Dipole-dipole forces, and Van der Waals interactions where the bonds can be easily broken [14]. The physical adsorption is basically a condensation process of adsorbate inside an adsorbent in which condensation heat of adsorbents is relatively similar to adsorption heat. Chemical adsorption relies on the chemical affinity of adsorbents to molecules of certain adsorbates. In this selective type of adsorption, the reaction of adsorbents and adsorbate results in formation of covalent bonds by either sharing or transferring of electrons. Different from physical adsorption, the adsorption molecules are decomposed during the desorption phase after chemical adsorption. Also, the adsorption/desorption heat is much larger in the chemical adsorption.

The physical adsorption is defined by the heat and mass transfer properties of adsorbents. For the desorption process, as the system pressure is high, the mass transfer process happens at a high rate due to high pressure, and therefore process is described by the heat transfer criterion. The chemical adsorption is influenced by the heat and mass transfer characteristics of the adsorbents, as well as the chemical reaction process and the reaction kinetics of the molecules. The adsorption uptake of chemical adsorbents is not limited by the surface area of the material, which generally leads to higher mass transfer kinetics in comparison to physical adsorbents [11]. However, chemical adsorption presents a challenge of products agglomeration and expansion which require large space volume in order to maintain high mass transfer performance. The most prevalent chemical adsorbents include metal chlorides, metal hydrides, metal oxides and salts hydrates [9], [11].

### **2.2. Adsorption refrigeration cycle**

The adsorption refrigeration cycle consists mainly of adsorption and desorption processes. An adsorption refrigeration cycle is driven solely by heat energy. An adsorption unit consists mainly of one or several adsorbers, a condenser, an evaporator, integrated with heat sources. Depending on the level of system continuity an adsorption cycle can be classified either as a basic cycle or an advanced cycle.

#### **i. Basic adsorption cycle**

A basic adsorption cycle comprises four steps: heating and pressurization, desorption and condensation, cooling and depressurization, and adsorption and evaporation. At first, the adsorber is heated by a heat source at a temperature  $T_H$ . The pressure of the adsorber increases from the evaporating pressure up to the condensing pressure while the adsorber temperature increases. In the second step, there's a continuous heating of the adsorber resulting in desorption of refrigerant vapors

from the contained adsorbent bed. This desorbed vapor is then liquefied in the condenser and the associated condensation heat is released to the first heat sink at a temperature of  $T_C$ . At the third step, the adsorber is at first disconnected from the condenser using a throttling valve. Then, it is cooled down by heat transfer fluid at the second heat sink temperature of  $T_M$ . This leads to a decrease in adsorber pressure from the condensing pressure down to the evaporating pressure proportionally to the decrease in the adsorber temperature. Lastly, the adsorber is connected to the evaporator and as the adsorber temperature keeps decreasing this leads to the adsorption of refrigerant vapor from the evaporator by adsorbent which consequently produces the desired cooling effect. The drawback of this type of cycle is its intermittent nature which implies the limitation of its application scope as the continuous cooling output is not attainable [25].

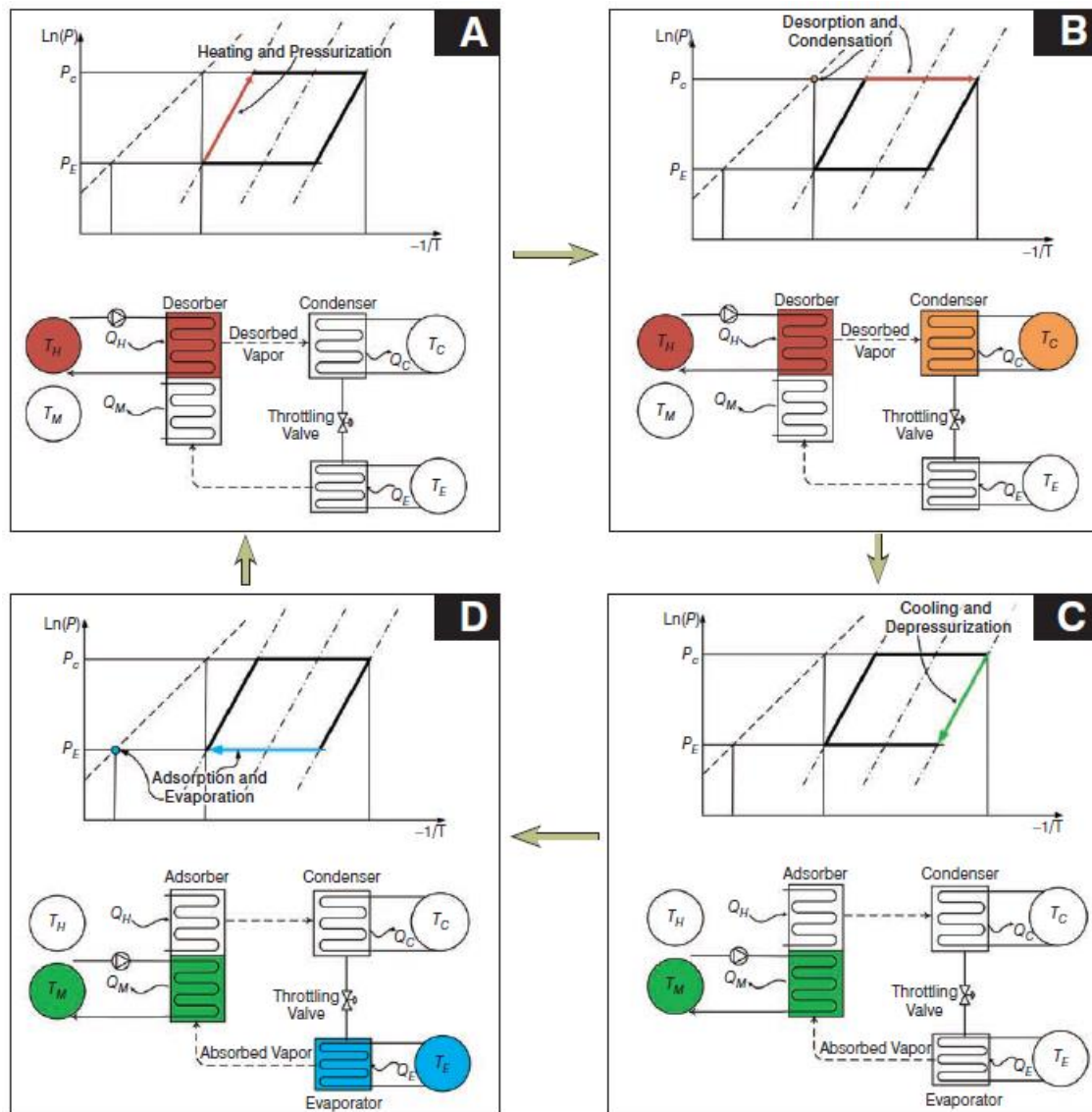


Figure 7 – Basic adsorption refrigeration system. A. Heating and pressurization. B. Desorption and condensation. C. Cooling and depressurization. D. Adsorption and evaporation [25]

## ii. Advanced adsorption cycle

The low efficiency and non-continuous operation mode of basic adsorption cycle have led to the search of more practical and efficient alternative cycles commonly classified under the label of advanced cycles. Among others the most applied cycles include: heat recovery cycle, mass recovery cycle and thermal wave cycle.

**The heat recovery cycle** – is used in a system with two or more adsorbers. It basically consists of an alternating set of cold and hot adsorbers. Following the end of the adsorption and desorption phases, the heat from the hot adsorber is transferred to the cold adsorber by circulating heat transfer fluid between them in a closed loop. The experimental results show that such system can improve the coefficient of performance (COP) up to 25% [26].

**The mass recovery cycle** – utilizes refrigerant mass within a closed loop of two connected high pressure and low pressure adsorbers to effectively increase system COP and the cooling effect. The refrigerant from the high-pressure adsorber is re-adsorbed by adsorbent in the low-pressure adsorber due to the pressure difference. In a mass recovery system, the overall adsorption quantity of adsorbent is increased, which consequently improves the cooling capacity and the system's COP up to 10% [26].

**The thermal wave cycle** – it is a two adsorber bed closed loop system that exploits the existing temperature gradient between adsorption and desorption phase using a heat transfer fluid to retain the lost heat. The heat transfer fluid circulates through system components. The adsorption heat released from the first adsorber bed is recovered by the circulating heat transfer fluid and then passed on to the second adsorber bed which subsequently leads low thermal energy consumption from the heat source. It is estimated that about 65% of the total energy received by each adsorber can be internally recovered [27].

## 2.3. Adsorption working pairs

The choice of appropriate adsorption working pair is an essential step in ensuring the highest possible performance for an adsorption refrigeration system. Desirable properties of adsorbents include high adsorption capacity over a wide range of temperatures, high heat and mass transfer and thermal stability. As for refrigerants the defining parameters are boiling point, melting point and relative pressures, vaporization heat, thermal conductivity, reactivity and stability, toxicity and environmental impact. The adsorption capacity of a working pair is usually determined graphically using isotherms. Using isotherms one can determine the adsorbate uptake amount per adsorbent unit mass as function of system pressure. The higher the adsorption capacity the higher the cooling effect an adsorption refrigeration system is likely to produce. This is due to the fact that adsorption capacity dictates the amounts of refrigerants that can be adsorbed and circulated in a cycle. In a given adsorbate-adsorbent system, the type of adsorption that takes place mainly depends on the surface reactivity, the nature of both adsorbate and adsorbent, and the temperature of adsorption. According to the nature of interaction between adsorbent and refrigerant, the adsorption working pairs are classed into three categories, physical, chemical and composite type.

### 2.3.1. Physical adsorbents working pair

The governing forces of physical adsorbents/refrigerants interaction are Van der Waal's forces. The most common working pairs of this type include: silica gel/water, zeolite/water, activated carbon/methanol, and activated carbon/ammonia.

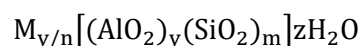
#### i. Silica gel and water pair

Silica gel is porous, non-hazardous and high thermally stable adsorbent with a high adsorption affinity to water vapor. Silica gel are commonly seen in desiccation applications due to its high adsorption ability. It is an amorphous and porous rigid, continuous net of colloidal silicon dioxide, composed of small grains of hydrated  $\text{SiO}_2$ . In principle it is prepared via the polymerization of a colloidal mixture of sodium silicate and silicic acid [13]. The hydroxyl group influences the polarity of silica gel as it can form hydrogen bonds with polar oxides like water and alcohol which makes it suitable for adsorption purpose. One hydroxyl can adsorb one molecule of water. The pore channel diameters of common silica gel are 2 nm, 3 nm for type A, and 0.7 nm type B silica gel. The specific surface area is about 100–1000  $\text{m}^2/\text{g}$ . the pore volume ranges in 0.3 – 0.4  $\text{cm}^3/\text{g}$ . By adsorption and capillary condensation silica gel can absorb water up to 40% of its weight. Much of silica gel's wide application is due to its non-corrosive and nontoxic nature.

The advantage of silica gel over other adsorbents is its low regeneration temperature of about 85°C which makes it suitable for intermittent low-grade thermal energy source applications like solar and waste heat powered adsorption refrigeration systems. In multistage refrigeration cycle systems, silica gel regeneration temperature can be as low as 50°C [11]. For non-regenerative systems with less components the dynamic losses can be avoided which in turn leads to higher COPs as there's no need to heat adsorbents to high temperatures. The desorption temperature needs to be controlled as the silica gel are destroyed in medium with temperatures over 120 °C. In comparison to activated carbons, silica gel exhibits higher adsorption heat of about 2500 – 2800 kJ/kg. At equilibrium, the maximum adsorption capacity to water ranges between 0.35 and 0.4 kg/kg silica gel with a low net instantaneous amount of adsorbate of below 0.1 kg water/kg silica gel under operating conditions [11]. The main limitation of silica gel/water system is the high freezing and boiling point of water which requires high vacuum pressure or water flow rates system to be applied for refrigeration purposes.

#### ii. Zeolite and water

Zeolites are hydrated aluminosilicate minerals made from interlinked tetrahedra of alumina and silica. Zeolite literally means “boiling rock” this due to its ability to trap water inside. There are over 200 known zeolites minerals of which about 40 are of natural occurrence and about 150 types zeolites which are artificially synthesized. The main types used for adsorption refrigeration purpose include chabazite, sodium chabazite, cowlesite, and faujasite. Artificially synthesized zeolites are named using one letter or a group of letters, such as type A, type X, type Y, type, ZSM Zeolites, etc [9]. Below is the general chemical formula of zeolite:



Where  $y$  and  $m$  are all integers and the ratio  $m/y$  is equal to or larger than 1.  $n$  is the chemical valence of positive ion of  $M$  and  $z$  is the number of water molecules inside a crystal cell unit.

The adsorption capacity of zeolites is dependent on the proportion ratio between  $Si$  and  $Al$ , and the smaller the ratio the higher the adsorption capacity. The zeolite selectivity is defined by its pore size and the common cage structure of the micropore could allow the adsorption process in a small range which explains the use of the term zeolite molecular sieve. The zeolite-water working pair has a wide range of desorption temperature of about 70–250°C. Due to its stable performance at high temperatures, zeolites are usually used in adsorption cooling systems with a high temperature heat source of between 200 and 300 °C [9]. In comparison to silica gel-water pair, zeolite-water exhibits higher adsorption heat of about 3300 – 4200 kJ/kg [11] which explains the low COP of such system.

### **iii. Activated carbon and methanol/ammonia pair**

Activated carbon is an adsorbent with high surface area derived from thermally or chemically treated (carbonization and activation) carbonaceous raw material. The common source materials are wood, peat, coal, fossil oil, char, bone, coconut shell, nut stone, and so on. Activated carbon has a hexagonal carbon atom ring shape with a specific surface area of between 500 and 1500 m<sup>2</sup>/g [9], [11]. The form and adsorption performance of activated carbon is dependent to the source carbonaceous material and preparation technique used. The adsorption performance is also influenced by the functional groups bonded to carbon atoms. The structure of activated carbon pores is comprised of irregular channels, with larger pore area at the surface of the grain, and narrow pore area within the grain. Activated carbon differs from other types of adsorbent mainly in its surface feature. Activated carbon surface is usually covered by an oxide matrix and other inorganic materials, which explains its weak polarity and low adsorption heat due to its susceptibility to decomposition processes.

In comparison with other physical adsorbents, activated carbon has a relatively low adsorption heat of about 1800 – 2000 kJ/kg, higher surface reactivity, wide range of pore size and large surface area. On the other hand, activated carbon has poor thermal conductivity in ranges near that of insulation materials [11]. Activated carbon-ammonia pair has a high working pressure around 1600 kPa at a condensation temperature of 40 °C which makes it applicable in sub atmospheric pressure systems. The main drawback of this working pair is the suffocating odor and toxicity of ammonia. As for activated carbon-methanol pair, such system presents a high adsorption capacity of 0.45 kg/kg adsorbent with low regeneration temperature of about 100 °C. However, the temperature should not surpass a 120 °C as in the presence of activated carbon, methanol decomposes into dimethyl ether at temperatures more than 150 °C [11].

### **2.3.2. Chemical adsorbents working pair**

Chemical adsorption working pairs are driven by chemical forces mainly complexation, oxidation, hydrogenation, and atom coordination at the surface layer between adsorbents and adsorbate. The most common chemical adsorbent-refrigerant pairs include metal chlorides–ammonia, metal hydrides–hydrogen, and metal oxides–oxygen [9], [11]. Chemical adsorbents have very large uptakes with specific adsorption capacity of about 1 kg/kg adsorbent, and desorption temperatures ranging between 40 to

80°C [11]. On the other hand, due to swelling and agglomeration processes prevalent in chemical adsorption, such systems have low stability which can hinder heat and mass transfer and consequently reduce the cooling effect they can produce. Consequently, chemical adsorbents are not as widely adopted as physical adsorbents in heat-driven chillers.

### **2.3.3. Composite adsorbents working pair**

The use of pure physical or chemical adsorbents system comes with the unique drawbacks associated with each type of adsorbent. For this reason, researchers around the world look at the composite form of adsorbents as a way to harness the unique positive attributes of both chemical and physical adsorbents in a one system. Composite adsorbents are developed synthetically by combining chemical adsorbents with a porous matrix. Porous components improve the heat and mass transfer performance of chemical adsorbents therefore limiting their agglomeration and swelling typical properties. On the other hand, the chemical adsorbents increase the overall adsorbate uptake capacity of the complex. Most common adsorbents composites are made by mixing of highly thermal conductive metal chlorides with activated carbon, expanded graphite, silica gel or zeolite. There three main techniques used in production of composite adsorbents: simple mixture, impregnation and mixture. In a simple mixture method, the chemical adsorbents are mixed with porous additive in a specific volumetric or gravimetric ratio. For impregnation method, the chemical adsorbent is first dissolved in a solvent, then the additives are added to the solution and later on dried to remove the solvent. The mixture (impregnation and consolidation) method consists of compressing the powder prepared by either of the other two methods [12].

### **2.3.4. Metal organic frameworks (MOFs)**

MOFs are organic-inorganic hybrid crystalline porous materials comprised of a regular array of positively charged metal ions surrounded by organic molecules. The metal ions form nodes that bind the organic elements together to form a cage-like structure. MOFs possesses large specific surface area up to 7800 m<sup>2</sup>/g. MOFs are designed based on the concept of reticular synthesis using an assembly of organic units and metal clusters as the building blocks to form robust complex structures [12]. In comparison to conventional adsorbents like silica gel and zeolites, MOFs presents a more flexible control in their definitive form and associated pores. Given their high porosity due to hallow nature and stability, among other applications, MOFs presents an interesting prospect to adsorption cooling applications especially heat pumps. The most common MOFs working pairs include MOFs – water, MOFs – ethanol and MOFs – methanol.

## **2.4. Adsorption equilibrium**

In an adsorbate-adsorbent system, the surface of adsorbent is exposed to adsorbate molecules. As the adsorbate molecules starts coming into contact with the adsorbent surface, some molecules stick to the surface and gets adsorbed while others rebound off. Initially the adsorption rate is higher as the relative available adsorbent surface is huge but with time as the molecules increase the available surface decreases and so does the rate of adsorption. Conversely, the desorption rate of molecules from covered surface starts to increase. With time, the rate of adsorption continues to decrease while the rate

of desorption increases until an equilibrium is reached between the two counter processes. At this stage the solid adsorbent is in adsorption equilibrium with the adsorbate molecules, as the rate of adsorption is equal to the rate of desorption. This is considered a dynamic equilibrium because the number of molecules sticking to the surface is equal to the number of molecules rebounding from the surface.

$$\frac{x}{m} = f(p, T) \quad \text{equation 1}$$

Broadly, for a given adsorbate-adsorbent system, the equilibrium amount adsorbed adsorbate per unit mass adsorbent ( $x/m$ ) is a function of pressure ( $p$ ) and temperature ( $T$ ). The adsorption equilibrium can be expressed in three different ways which are: adsorption isotherms, isobars and isosteres.

i. **Adsorption isotherm:** is a graphical representation of the variation in the amount of adsorbate adsorbed on the surface of a unit mass adsorbent with the change in pressure at a constant temperature.

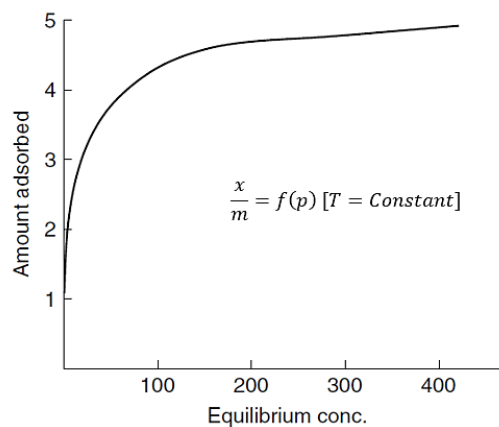


Figure 8 – Adsorption isotherm

ii. **Adsorption isobar:** with pressure kept constant and the temperature as a variable, the equilibrium of adsorbate-adsorbent system is represented by an isobar.

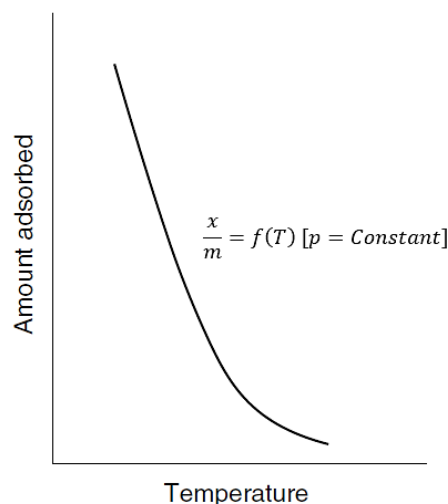


Figure 9 – A typical adsorption isobar

iii. **Adsorption isostere:** at a constant adsorption amount ( $x/m$ ), the function relating the equilibrium pressure to the temperature is called isostere.

### 2.4.3. Types of adsorption isotherms

In practice of the three methods, adsorption isotherm is the most widely adopted method in interpreting adsorption performance of different adsorbate-adsorbent systems as the study of adsorption process at a specific temperature is a more pragmatic approach especially within the scope of cooling systems. From the kinetics perspective, according to IUPAC (International Union of Pure and Applied Chemistry), adsorption isotherms can be classified into six types of isotherms.

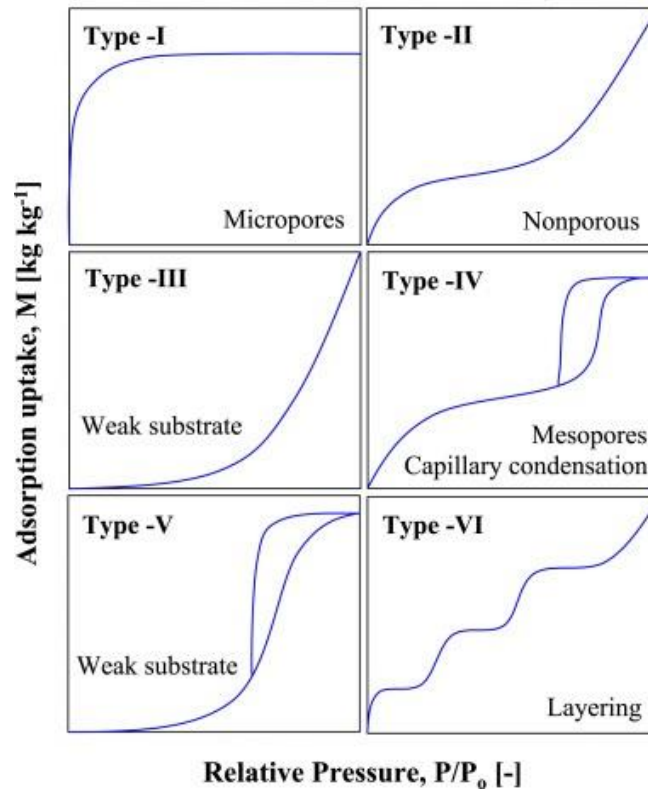


Figure 10 – Classification of adsorption isotherms according to IUPAC

**Type I** – This isotherm is typical for microporous system with strong adsorbate-adsorbent activity. It is characterized by a horizontal plateau indicative of a monolayer system which it maintains as the gas pressure increases. Type I curve corresponds to the Langmuir adsorption model.

**Type II** – Typical for physical adsorption on macro-porous or non-porous material. Type II isotherm exhibits a continuous increase in adsorbate uptake trend as the relative pressure increases towards a unit ratio without any plateauing phenomena [18]. It depicts adsorption on mesoporous monolayer materials at low pressure and on mesoporous multilayer material at high pressure near saturation with no hysteresis. It has one inflection point. Moreover, its observed in only microporous, nonporous, or disperse solids with > 50 nm pore diameter [14].

**Type III** – This isotherm characterizes systems where the interactions between adsorbate molecules are higher compared to adsorbate-adsorbent interaction. The adsorbate uptake increases exponentially with increasing pressure. Such system is associated with formation of multiple layers and exhibits adsorption heat which is lower than condensation heat.



**Type IV** – This isotherm type characterizes adsorption patterns in mesoporous medium. Type IV isotherm combines the characteristics of both Type II and Type I isotherms. It has an intermediate saturation of adsorption surface at the low pressure and at higher pressure, the adsorption uptake again experiences saturation near the saturation pressure [18]. It is an irreversible type of adsorption as it exhibits multilayer formation capillary condensation with a hysteresis phenomenon between the adsorption and the desorption branch. Capillary condensation refers to the phenomenon whereby gas vapour condenses at partial vapour pressure below saturation pressure. It enables vapour liquefaction in porous materials at low vapour pressures. It depends on pore geometry, the smaller the pores the lower the condensation vapour pressure.

**Type V** – This adsorption isotherm exhibits similar mechanism as Type III, the intermolecular cohesive force in adsorbate bulk is higher than the adhesive force between adsorbate-adsorbent molecules. The Type V isotherm present an S-shaped characteristic, comprising three distinctive uptake rates. At low pressure, the uptake rate is gentle and then a steep rise at intermediate pressure, which then followed by a plateauing of uptake at higher pressure. It is common in mesoporous materials with a desorption pattern of type IV isotherm resulting from capillary condensation. Typical example for such isotherm is seen in adsorption of water on carbon molecular sieves and on activated carbon fiber [14].

**Type VI** – It is a complex type of isotherm with a stepwise multilayer adsorption. It occurs only when the sample surface contains different types of adsorption sites with energetically different characteristics. Typical example is the adsorption of noble gases on the surfaces of planar graphite, and adsorption of butanol on aluminum silicate, adsorption of methane ( $\text{CH}_4$ ) on magnesium oxide ( $\text{MgO}$ ) [14].

## **2.5. Potential advantages and limitation challenges facing the use of adsorption chillers**

Interest in adsorption chillers have gained traction due to the promise of positive environmental impact this technology can potentially bring in contrast to the alternatives. Nonetheless the slow commercial adoption of adsorption cooling solutions is staggering. The current technical limitations of adsorption chillers mainly its low COP puts it in a disadvantageous position to commercially compete for market against the absorption and compression refrigeration solutions.

The use of adsorption chillers presents several advantages including: the low electricity consumption hence potentially the decrease of the load on the power grid if widely adopted; the possibility that adsorption systems can be powered by waste heat, solar energy and potentially geothermal energy has a net positive environmental impact; lack of moving parts or vibrations and low level of noise; the ozone depletion neutrality of the working fluids medium applied in these systems. However, the adoption of adsorption chillers faces technical challenges mainly the low COP of the current available systems. For an adsorption chiller to be economically viable it has to be powered by a renewable energy or waste heat source [28]. The cyclic operation mode of adsorption chillers results in an irregular intermittent cold production. The other challenge is the large size and mass of adsorption chiller systems. An important hurdle facing the adoption chillers is the fact that its overall investment cost is much higher than that of alternative solutions [28].

### 3. A REVIEW OF ACTIVATED CARBON: USE AND PRODUCTION

The use of carbon dates so far back in time that its origin is impossible to point to exactly. Prior to the use activated carbon, wood char, coal char or partially devolatilized carbonaceous material were utilized as an adsorbent. The first reported application of activated carbon as a gas phase adsorbent was firstly recorded in 1793, when Dr. D.M. Kehl applied wood char in order to mitigate the odours emanating from gangrene an application he then recommended for water filtration [15]. From then on activated carbons saw applications in sugar production industry as decolorizing agents, sewer ventilation systems as piquant odours mitigating agents. However, the significant development in production and applications of activated carbon gained a boost during the First World War when poisonous gases warfare by the Germans forced the Allies Army to come up urgently with gas masks solution [15]. The second half of the 20<sup>th</sup> century saw an increase of interest in research and development of activated carbons for food, chemical processing, solvent recovery and industrial gas treatment [36] due to several factors mainly ever stringent environmental regulations and public consciousness of the potential role the activated carbons can play in efforts to mitigate the negative impacts imposed by other industrial chemicals applied in different applications.

#### 3.1. Properties of activated carbon

Activated carbons are highly developed porous carbon structures which contains heteroatoms and some minerals. The core properties of activated carbons are defined by the raw materials they are derived from coupled with the methods deployed in their preparation. As any other substance, the activated carbons exhibits both physical and chemical properties. The chemical properties of activated carbons are substantially dictated by the surface groups formed by its heteroatoms. For the purpose of physical adsorption, thermo-physical properties are of the utmost interest to us in this work. According to IUPAC, the porous structure of activated carbons can be classified in three groups: *micropores*, *mesopores* and *macropores*.

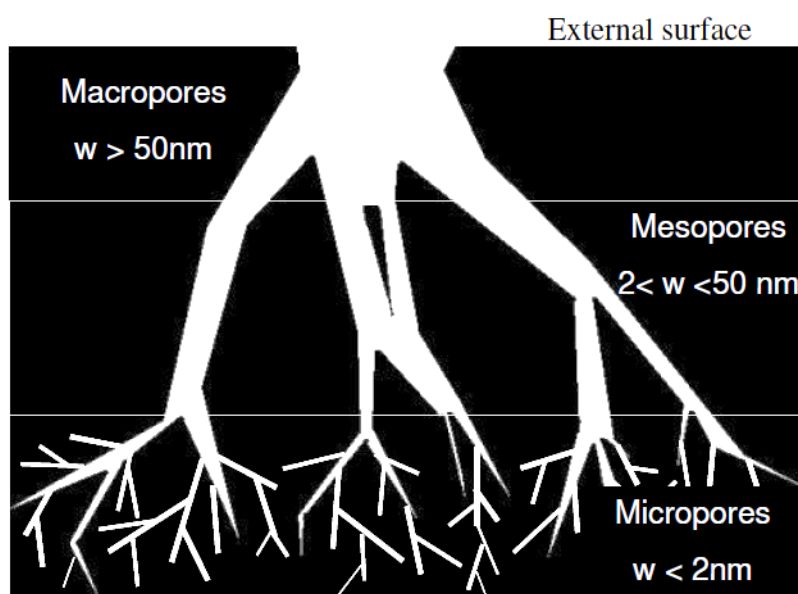


Figure 11 - Pore structure network of activated carbon [15]

### ***i. BET surface area***

Adsorption is a surface process. Hence the specific surface area of an activated carbon is of a parameter of key importance for adsorption applications. The specific surface area is often determined by applying the BET equation to adsorption isotherms of a given system. BET determination is based on the Langmuir monolayer molecular adsorption theory. Commonly this done through isotherms generated from adsorption of N<sub>2</sub> at 77 K or CO<sub>2</sub> at 273 K [15]. The calculation of a BET specific surface area is a multistep process which goes as follows:

At first monolayer adsorbed gas volume ( $v_m$ ) is determine using the below BET equation 1

$$\frac{1}{v[(p_0/p) - 1]} = \frac{c - 1}{v_m c} \left( \frac{p}{p_0} \right) + \frac{1}{v_m c} \quad \text{equation 2}$$

Where:  $v$  – adsorbed gas quantity,  $p_0$  – adsorbate saturation pressure,  $p$  – adsorbate equilibrium pressure,  $C$  – BET constant ( $C = \exp[(q_1 - q_L)/RT]$ ),  $q_1$  – adsorption heat for the first layer,  $q_L$  – vaporization heat.

Then using the monolayer adsorbed gas volume ( $v_m$ ), the total and specific surface area are determined from the following equations:

$$S_t = \frac{v_m N s}{V} \quad \text{equation 3}$$

Where:  $S_t$  – the adsorbent sample total surface area,  $N$  – Avogadro's number ( $6.02 \times 10^{23} \text{ mol}^{-1}$ ),  $s$  – cross-sectional area of adsorbed gas molecule,  $V$  – molar volume of adsorbed gas.

$$S_{BET} = \frac{S_t}{a} \quad \text{equation 4}$$

Where:  $S_{BET}$  – specific surface area,  $a$  – adsorbent sample mass

For activated carbons the range of linearity of the BET plot is restricted to the  $p/p_0$  range of 0.05-0.20. The BET equation surface area characterization faces limitations when analyzing microporous activated carbon. The microporous network may give rise to molecular sieving and selectivity depending on the adsorbates used. Hence both adsorption of N<sub>2</sub> at 77 K or CO<sub>2</sub> at 273 K are used complementarily in characterizing activated carbon in order to mitigate limitations each possesses [15].

The BET surface area for activated carbons commonly ranges between 500 to 1500 m<sup>2</sup>/g but values can be even higher in some cases. Most of adsorption takes places in micropores, about 90-95% of the total surface area of an activated carbon are attributed to micropores. Depending on the size of adsorbate molecules, at times the mesopores act as channels conducting the adsorbates from micropores to macropores and vice versa [15]. This also illustrates the effect pore size distribution can have on adsorption capacity of adsorbents.

### ***ii. Surface chemistry of activated carbon***

Surface area and pore size distribution are not the only adsorption performance determining factors for activated carbons. Analogous textural properties of different activated carbon samples do not guarantee

same adsorption capacity for both samples on the same adsorbate. This can be explained by the intrinsic difference of the samples together with their surface groups in other words their difference in surface chemistry. Unpaired electrons present in activated carbons are usually bonded to heteroatoms giving rises to surface groups. Oxygen containing surface groups are the most prevalent in activated carbons. Below is a figure with other surface groups that are commonly found in activated carbon.

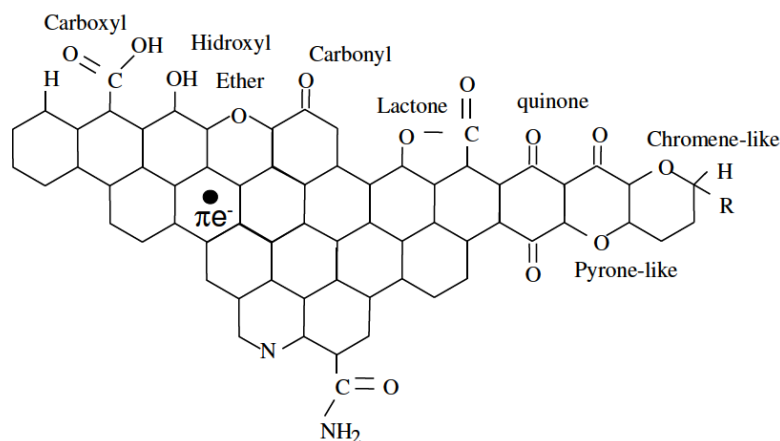


Figure 12 – Surface groups commonly found in activated carbons [15]

Surface groups account for a small ratio of the total surface area found in activated carbons however their influence on adsorption capacity due to their chemical properties cannot be understated. The presence or absence of one or several surface groups in an activated carbon can alter to a great extent its adsorption performance on a given adsorbate. The influence of surface groups on adsorption capacity of activated carbons manifests mainly in two ways, by changing the hydrophilicity and altering the acidic/basic tendencies of activated carbons which are intrinsically both hydrophobic and amphoteric.

### 3.2. General production process of activated carbon

Activated carbons are produced from isotropic, non-graphitic and non-graphitizable carbonaceous materials. Graphitizability refers to the ability of carbons to develop graphitic structure following graphitization heat treatment [16]. Selection of activated carbon precursors is tailored to the end applications as the raw materials together with production treatment has a high influence on activated carbon performance. The key criteria in selecting precursors carbonaceous materials include the following: *high density and hardness (carbon content), low inorganic matter content, availability and cost*. Generally, wood, coconut shells, fruit stones, coals, lignite, petroleum coke are all cheap materials with a high carbon content and a low inorganic content, and consequently, are widely acceptable for use as an activated carbon precursor [15]. Production of activated carbon involves an important stage of activation. Activation is carried out mainly to increase the number of pores and sizes of the existing ones to ensure high possible adsorption capacity is attained. The different activation processes are divided into two groups: *chemical and physical activation*. The main differences between both are the procedure and the activating agents applied [37].

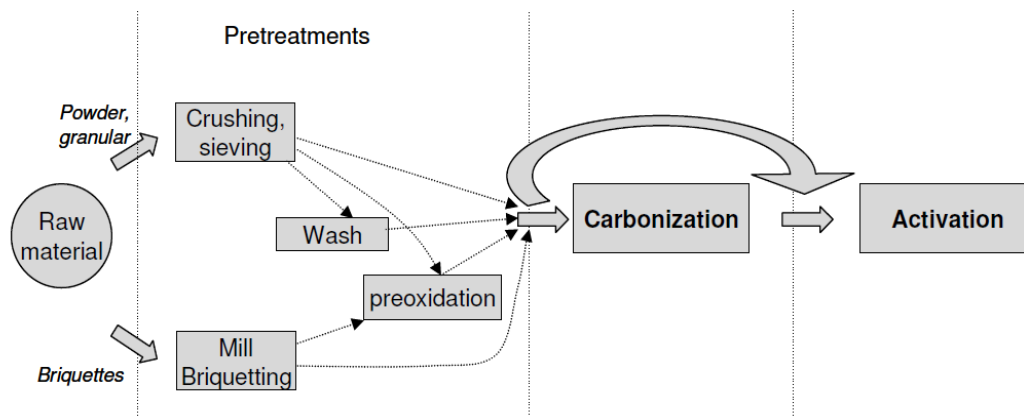
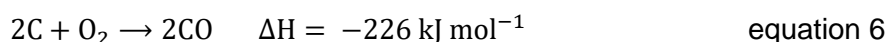
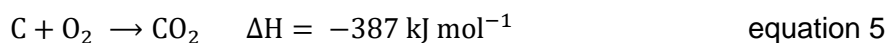


Figure 13 – General industrial flow chart for the production of thermal activated carbons [15]

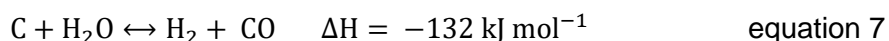
### 3.2.1. Physical activation of activated carbon

Physical activation is a two-step process that basically consists of devolatilization of precursors combined with char gasification by an oxidizing agent. It involves a carbonization (pyrolysis) step in an inert atmosphere. Thermal carbonization of precursor carbon material results in char rich in carbon which then undergoes activation with oxidizing agents such as steam, carbon dioxide and nitrogen within a temperature range of 800–1100 °C [19]. This chemical free and inexpensive approach has ability to produce activated carbon of porous structure with relatively hard strength. However, it exhibits disadvantageous traits of activated carbons with low adsorption capacity, long activation duration, and high energy consumption [19]. The most common agents and reaction schemes applied in thermal activation are presented below [15]:

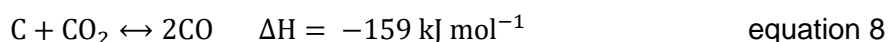
#### i. Activation with oxygen



#### ii. Activation with steam



#### iii. Carbon dioxide activation



### 3.2.2. Chemical activation of activated carbon

Chemical activation involves inert carbonization of a mixture of precursor material with a chemical agent. The mixing of the precursor raw material and the chemical agents is done either via impregnation or physical mixing [19]. This approach is commonly used for cellulose containing raw material. Different from thermal activation, in chemical activation the carbonization and activation steps occur concurrently which implies the possibility of a single furnace process. Here either the raw precursor material or its previously carbonized product is impregnated with suitable chemical agents depending on the end application, such as acids ( $\text{HNO}_3$ ,  $\text{H}_2\text{SO}_4$ , and  $\text{H}_3\text{PO}_4$ ), alkali hydroxides ( $\text{NaOH}$  and  $\text{KOH}$ ) or salts ( $\text{ZnCl}_2$ ,  $\text{MgCl}_2$ ,  $\text{FeCl}_3$ ,  $\text{AlCl}_3$ , and  $\text{K}_2\text{S}$ ) [20]. Then the resulting suspension is dried and the remaining mixture is heated for a given time. The choice of activation temperature usually ranging between 400 to 900 °C, is dictated by the activating agent and the desired properties of the final product [19]. The

properties of the final activated carbon are mainly influenced by the gravimetric ratio of activating chemical agents to the raw dry precursor. In comparison to physical activation, chemically activated carbons exhibit higher porous structure and subsequently more BET surface area [19]. Hence chemical activation is commonly the most preferred method over physical activation as besides the high-quality activated carbons it produces, it is also the faster process with relatively lower activation temperature [21].

#### ***Potassium hydroxide activation of activated carbon***

Alkali hydroxides like potassium hydroxide (KOH) are commonly used for activation of coal-based precursors in our case spruce lignin [19]. Among various available chemical activators, KOH is widely considered the method of choice in production of low cost activated carbon [21]. In the 1980s, Amoco Corporation developed a process to produce high surface area carbons (over 3000 m<sup>2</sup>/g) by the KOH activation of aromatic precursors such petroleum coke and coal. The activated carbon is predominantly microporous, subsequently resulting in high surface area, and the total pore volume is exceptionally high: 2.0–2.6 mL/g [22]. It is well established that activated carbons produced via KOH activation are highly microporous in comparison to those produced through ZnCl<sub>2</sub> or H<sub>3</sub>PO<sub>4</sub> activation [21]. KOH activation approach aims to produce activated carbon with a narrow pore size distribution and the development of effective porosity. It is believed that the activation mechanism with alkali metals such as KOH relies on the fact that alkali metals act as an input catalyst in the carbon network, an electron donor, during the gasification reaction [23].

## 4. EXPERIMENTAL METHODS AND PROCEDURE

The adsorption of methanol on activated carbon and potential applicability of the studied samples to adsorption chillers was the focus of this work. This chapter details the selection of the adsorbate – adsorbent system. The preparation method and treatments of the studied adsorbent samples are explained. The characterization of thermo-physical properties of adsorbent are also highlighted in this chapter. The experimental setup of the sorption performance analyzer is also explained in this section.

As recommended in literature, the search for a suitable adsorbent for adsorption cooling application has to be based on the following key considerations [29], [30]:

- i. Adsorbent should have high enough adsorption capacity under low temperature conditions and also ability to release adsorbates when thermal energy is supplied to the bed.
- ii. Adsorbent should exhibit high latent heat of adsorption compared to sensible heat.
- iii. Adsorbent should be mechanically stable under use.
- iv. Non-toxic and non-corrosive to ensure a net zero ecological impact over its use life cycle
- v. For feasibility purpose, adsorbents should be widely available and relatively cheap.

Activated carbon meets most of the above listed adsorbents viability criteria as it offers high adsorption capacity, low cost, availability, large surface area, an easy-to-design pore structure, hydrophobicity (insensitiveness to moisture), and low energy requirements for regeneration. Which are all essential parameters to consider for applicability and viability of any given adsorbent.

### 4.1. Preparation and treatment of studied activated carbon samples

In this study three activated samples were considered and the comparative analysis of their methanol adsorption performance was made. The two of the samples CWZ22 and CWZ22P are commercially available activated carbon samples obtained from “CARBON” branch of the company ELBAR – KATOWICE Sp. z o. o. These are produced based on charcoal precursor materials and are activated by steam. The third sample is WA TONG activated carbon produced from lignin. The WA TONG sample was experimentally produced at AGH by Dr. Sztekler and his colleagues from spruce derived lignin precursor material and was activated chemically using potassium hydroxide KOH. The preparation method and activation procedure applied are described below:

- i. Kraft lignin produced from spruce by the CleanFlow Black Lignin (CFBL) process was used as the carbon precursor material [24]. Before the experiment, the lignin was first dried at room temperature to a moisture content level of about ~2%. Then the dried lignin was grinded and sieved to the size of particle diameter  $d < 0.125$  mm.
- ii. 10 g of kraft lignin was then mechanistically mixed with 1.9 g  $\text{FeSO}_4$ .
- iii. The resulting mixture then underwent carbonization at 550 °C for 1 hour.
- iv. Followed by mixing of Fe-hydrochar product with KOH (1:3 ratio) by way of mechanical stirring overnight at room temperature.
- v. Then the mixture was dried at 105 °C.

vi. Followed by activation at 800° C for a duration of 3 hours.

vii. The resulting product was then washed using distilled water until pH reach to neutral levels and then drying of the product at 95 °C in an oven for 24 hours duration.

#### **4.2. Choice of adsorbate for the activated carbon system**

The performance of an adsorption cooling system is mainly predicated on the adsorbent adsorbate pair system applied. The key parameters for this assessment are the specific cooling power (SCP) and the coefficient of performance (COP). SCP is predefined by the adsorption capacity of an adsorbent to a given adsorbate in a particular set of conditions (Temperature and pressure). Ideally an adsorbate should meet the following criteria for an adsorption system to be viable and robust [29],[30]:

- i. An adsorbate should have the boiling point below 0 °C.
- ii. To maximize the adsorbent adsorption intake, it should have small molecular size.
- iii. High latent heat of vaporization and low specific volume.
- iv. Thermally stable with the adsorbent to ensure a wide range of cycle operating temperature.
- v. Non-toxic, non-corrosive and non-flammable for both safety and ecological rigour.
- vi. Low saturation pressures at normal operating temperature.

As non-polar adsorbent, activated carbon exhibits hydrophobic properties. Hence in adsorption cooling applications, ammonia (NH<sub>3</sub>) and methanol (CH<sub>3</sub>OH) are two adsorbates commonly paired with activated carbons.

Given its large adsorption capacity and low adsorption heat of about 1800 to 2000 kJ/kg, activated carbon – methanol pair has potential to be widely used in practical systems. As the majority of energy consumed in the desorption phase is the adsorption heat, it is beneficial to the system's COP to have a pair with relatively low adsorption heat [25]. Also, methanol's properties of high latent heat of evaporation and low freezing point below that of water, make the activated carbon – methanol system suitable for low-grade heat source applications within the range of about 70 to 120 °C [17]. However, it is important to note that any system of temperatures higher than 120 °C will lead to decomposition of methanol into dimethyl ether (CH<sub>3</sub>OCH<sub>3</sub>) [25]. Typical working pressure for an activated carbon – methanol system is sub-atmospheric; hence a hermetically sealed outer vessel is required. Methanol of purity 99.90% (Methanol for LC-MS CHROMASOLV® [67-56-1]) was used as the adsorbate of choice to pair with activated carbon for this study.

Activated carbon – ammonia system exhibits almost similar adsorption performance to activated carbon – methanol system. However, the two systems differ in that activated carbon – ammonia is a positive pressure system with possibility of using higher temperature heat source 200 °C and above [25]. The major drawback of such system are the high toxicity and pungent smell of ammonia. In this study the adsorbate of choice is methanol for the above stated advantages as it fits our purpose of exploring the potential of cooling generation using low-grade heat source.



### 4.3. Characterization of the samples

Given the chemical and structural non-homogeneous nature of activated carbons, characterization of such porous samples is a complex process and it usually involves a combination of various methods to fulfill this purpose [37]. The characterization was carried with the goal to learn the distinctive textural and thermo-physical properties of the samples. However, this was not fully achieved as there are few crucial sample properties like BET surface area, chemical surface composition and surface morphology imaging that were not performed due to different work limitation factors. Porosity, pore volume, density and crystal structure analysis of the samples are presented next.

#### 4.3.1. Porosity, Pore volume, True and Apparent density of the samples

As a porous material, activated carbon samples have both apparent density and true density. Both properties were measured for all three studied samples. Analytical technique of gas displacement pycnometry (AccuPyc II helium pycnometer) was used to determine the true density of the samples. True density was determined based on the skeletal volume of the sample measured through helium displacement penetrating into the open pores in the studied lump sample. By the method of pycnometer quasi-liquid displacement apparent density was determined. A GeoPyc 1360 quasi-liquid pycnometer was used for this. The test consisted in determining the volume of a lump sample in dry conditions.

Porosity ( $\varepsilon$ ) was estimated from the obtained sample apparent ( $\rho_b$ ) and true ( $\rho_p$ ) density through the equation below:

$$\varepsilon = (1 - \rho_b / \rho_p) \times 100 \quad \text{equation 9}$$

Pore volume of the samples was determined from the following relation:

$$\text{Pore volume} = \frac{\varepsilon}{100} \times \frac{1}{\rho_b} \quad \text{equation 10}$$

Table 2 – Sample density, porosity, and pore volume analysis results

Sample	nr	True density, g/cm <sup>3</sup>	Apparent density, g/cm <sup>3</sup>	Porosity, %	Pore volume, cm <sup>3</sup> /g
WA TONG	1	2.1055	0.8070	61.67%	0.76
	2	2.1026	0.8475	59.69%	0.70
	<b>average</b>	<b>2.1041</b>	<b>0.8273</b>	<b>60.68%</b>	<b>0.73</b>
CWZ22P	1	1.6572	0.6314	61.90%	0.98
	2	1.6579	0.6653	59.87%	0.90
	<b>average</b>	<b>1.6576</b>	<b>0.6484</b>	<b>60.89%</b>	<b>0.94</b>
CWZ22	1	2.0483	0.4353	78.75%	1.81
	2	2.0848	0.4590	77.98%	1.70
	<b>average</b>	<b>2.0666</b>	<b>0.4472</b>	<b>78.37%</b>	<b>1.75</b>

### 4.3.2. X-Ray Diffraction analysis

The phase composition and crystal structure analysis of the considered powdered activated carbon samples were done at room temperature using the powder X-ray diffraction method (XRD) with CuK $\alpha$  radiation. Panalytical Empyrean diffractometer equipped with PIXcel3D detector was used, with the  $2\theta$  angular range of 10-110 degrees, a  $2\theta$  step size of 0.013 degrees and a scan step time of 97 seconds.

In principle XRD technique involves diffraction of X-Rays off the sample material whereby the signal is recorded and graphed with emerging peaks highlighting the relative atomic structural differences existing within the sample. The obtained XRD monographs for the three samples WA TONG, CWZ22 and CWZ22P are presented below.

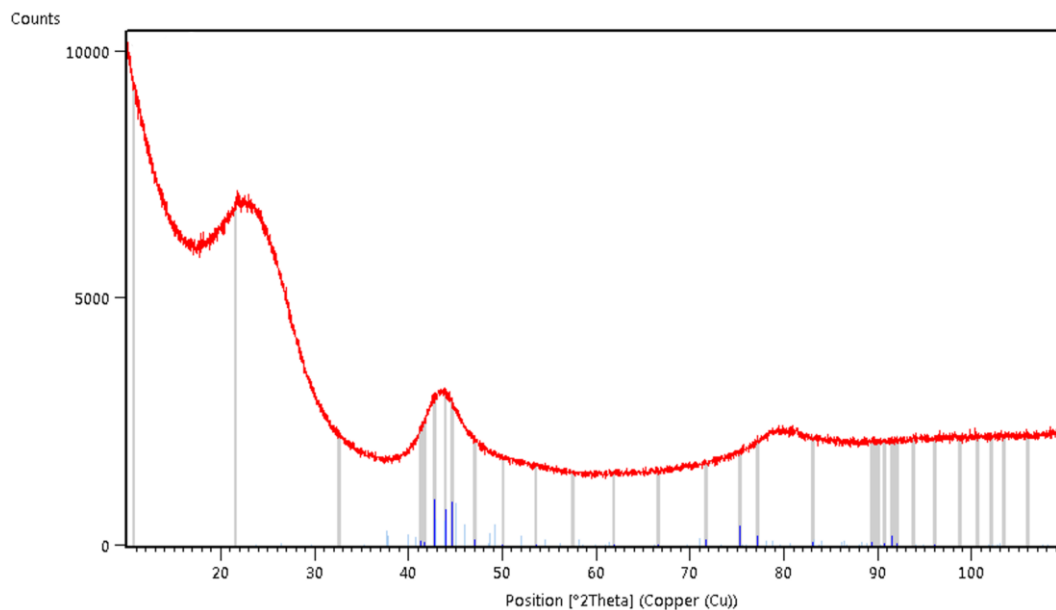


Figure 14 – XRD pattern of CWZ22 sample

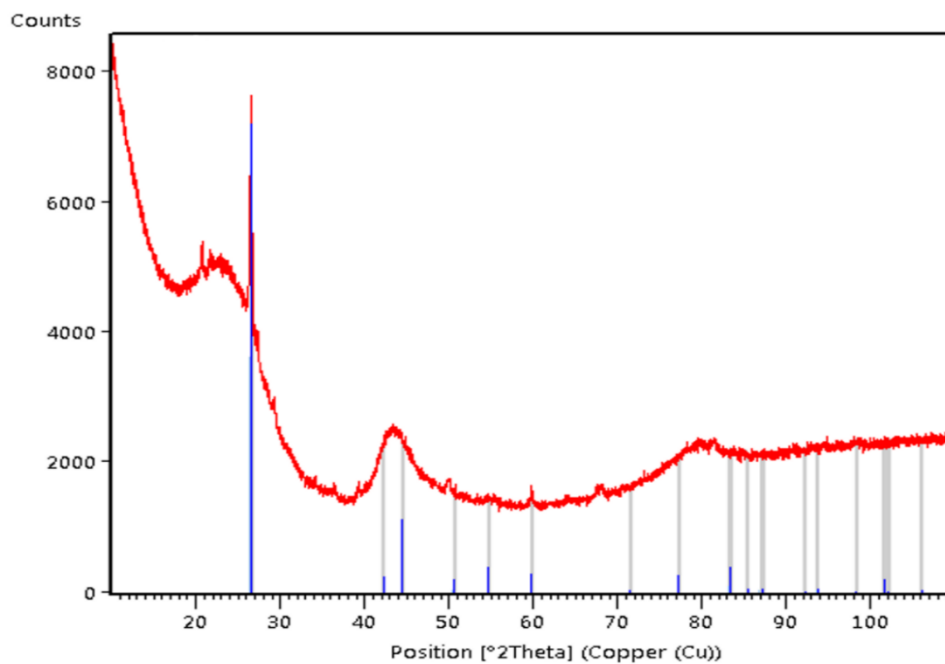


Figure 15 – XRD pattern of CWZ22P sample

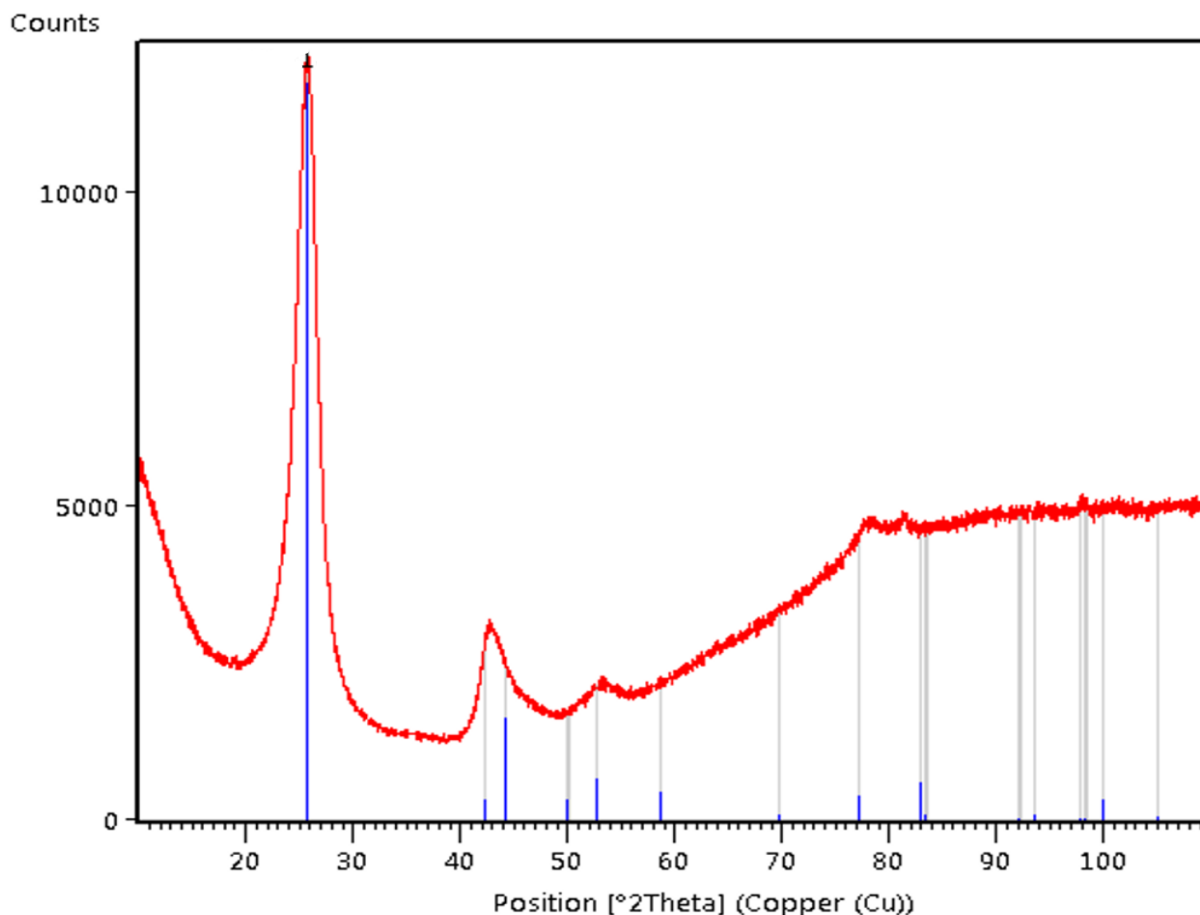


Figure 16 – XRD pattern of WA TONG sample

The presence of diffraction sharp peaks on the above XRD graphs is indicative of the existence of a well aligned layer of crystalline carbonaceous structure in all three studied samples [35]. On all obtained monographs the noticeable strong and weak diffractions peaks appear around 2Theta ( $2\theta$ ) degree positions of 25 and 45 respectively. WA TONG sample exhibits sharper diffraction peaks than the commercial samples (CWZ22 and CWZ22P), this indicate that WA TONG sample has bigger crystallite size [34]. The almost nonexistence of many sharp peaks across obtained monographs informs that all three samples are predominantly of amorphous structure [35]. The lower crystallinity level in the sample, the more amorphous structure of the samples and consequently the higher probability of having larger specific surface area which is a preferred feature for adsorption application [34].

#### 4.4. Experimental setup of the sorption performance analyzer

The sorption performance of activated carbon samples was studied using the novel Dynamic Vapor Sorption (DVS) vacuum analyzer. It is based on the principle of gravimetric analysis of the sample whereby the sorption properties of a sample like activated carbon are measured in a preset condition (pressure and initial temperatures) as a controlled flow of a given adsorbate passes through the sample accompanied with monitoring intime weight change of the sample. In the study of the activated carbon samples, the DVS analysis operates in a continuous open flow cycle.

In this experiment, before opening the DVS chamber to set up the samples the system pressure was levelized with the room atmospheric pressure using the pump control valve at the rate of 0.1 torr/s up to 10 torr (10 mmHg) and then at rate of 1 torr/s till to the room atmospheric pressure of about 750 torr was reached. Then the activated carbon sample mass of about 20 mg was measured and placed on the sample slide paired with an empty control reference pan inside the chamber. The vapor flask was filled with methanol as it is the adsorbate choice for the study. After the chamber is sealed tight and the pump atmospheric valve is closed. Then the rotary pump is turned on to create vacuum in the system.

The sorption analysis for each sample were carried out on four different adsorption temperature points (30, 40, 50 and 60 °C) depending on which the saturation vapor pressure for methanol were set in the predefined DVS software method with a set of parameters like system temperature, process time duration together with step increment, and adsorbate vapor flow rate. In our case these parameters included preheating and cooling for 60 minutes each and sorption timestep duration (20 minutes per increment). After setting up the sample and making sure the vacuum state is assured in the system. The process starts with drying and in-situ degassing of the sample (preheating), followed by an about hour cooling of the sample to the predefined temperature point, and then the adsorption process starts with adsorption rate varying incrementally with the relative pressure change in the system till the adsorbate saturation pressure is reached at P/Po of 100% the point at which maximum desorption rate and minimum adsorption rate are observed. The analysis results were obtained in form of adsorption isotherms and adsorption kinetics curves.



Figure 17 – DVS Vacuum gravimetric sorption analyzer [38]

## 5. RESULTS AND DISCUSSION

### 5.1. Adsorption performance analysis results

The adsorption analysis was performed by DVS method. Three activated samples' adsorption performance on methanol were put to test under vacuum condition. The experiment was carried out at four different temperature points (30, 40, 50, and 60 °C) for each sample and a DVS method was predefined in accordance with the methanol saturation pressure ( $P_o$ ) at each of the four points. The results of this analysis are illustrated in form of adsorption isotherms and kinetics curves.

#### 5.1.1. Synthesized spruce-based sample – WA TONG

At adsorption temperature 30 °C, reference sample weight - 21.047 mg, methanol saturation pressure at 30 °C - 21.83 kPa

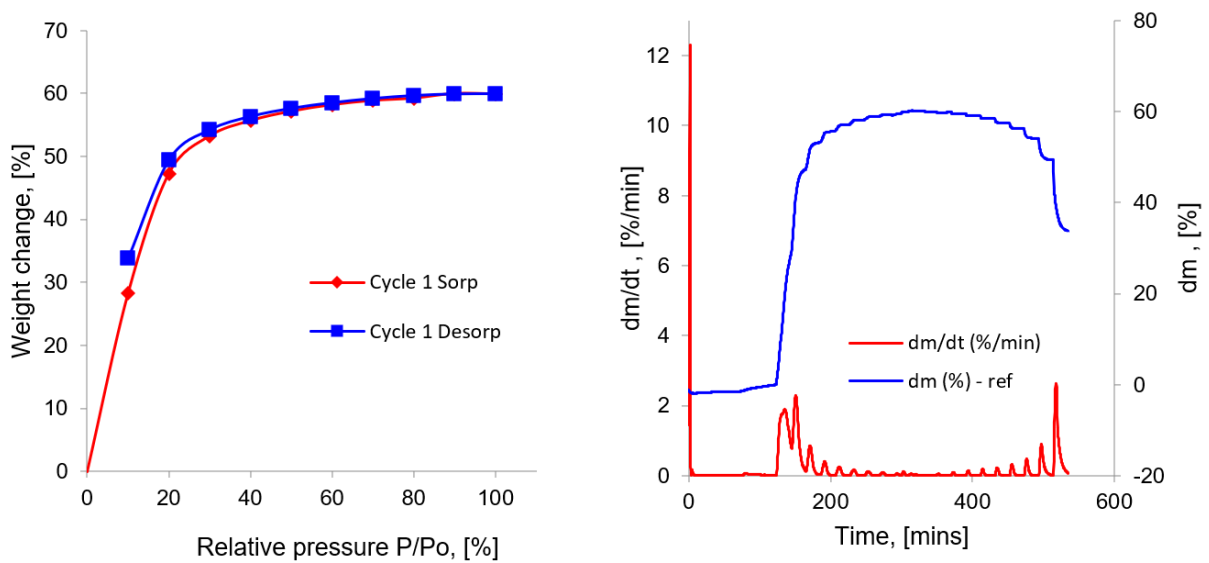


Figure 18 – Methanol adsorption on WA TONG at 30 °C. a) isotherm, b) kinetics

At adsorption temperature 39.7 °C, reference sample weight – 5.039 mg, methanol saturation pressure at 40 °C - 35.38 kPa.

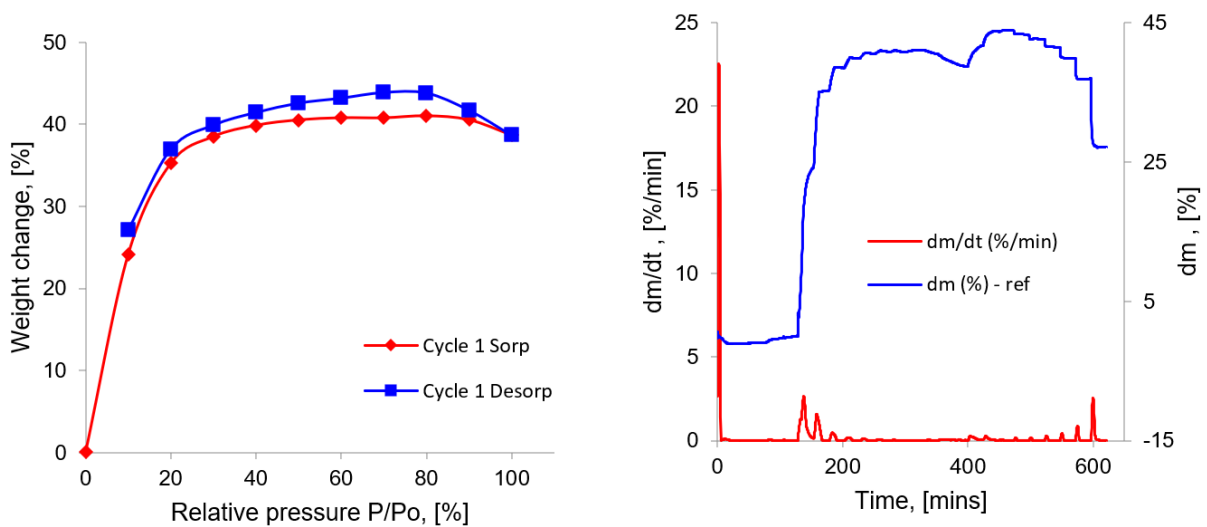


Figure 19 – Methanol adsorption on WA TONG at 40 °C. a) isotherm, b) kinetics

At adsorption temperature 49.3 °C, reference sample weight – 5.25 mg, methanol saturation pressure at 50 °C – 55.47 kPa.

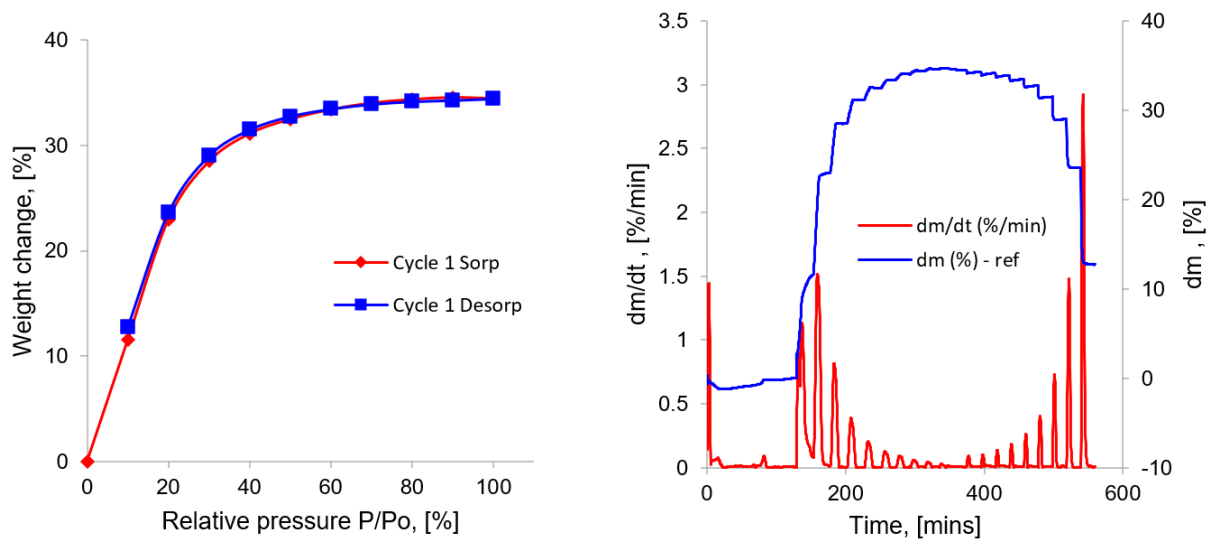


Figure 20 – Methanol adsorption on WA TONG at 50 °C. a) isotherm, b) kinetics

At adsorption temperature 58.8 °C, reference sample weight – 5.49 mg, methanol saturation pressure at 60 °C – 84.40 kPa.

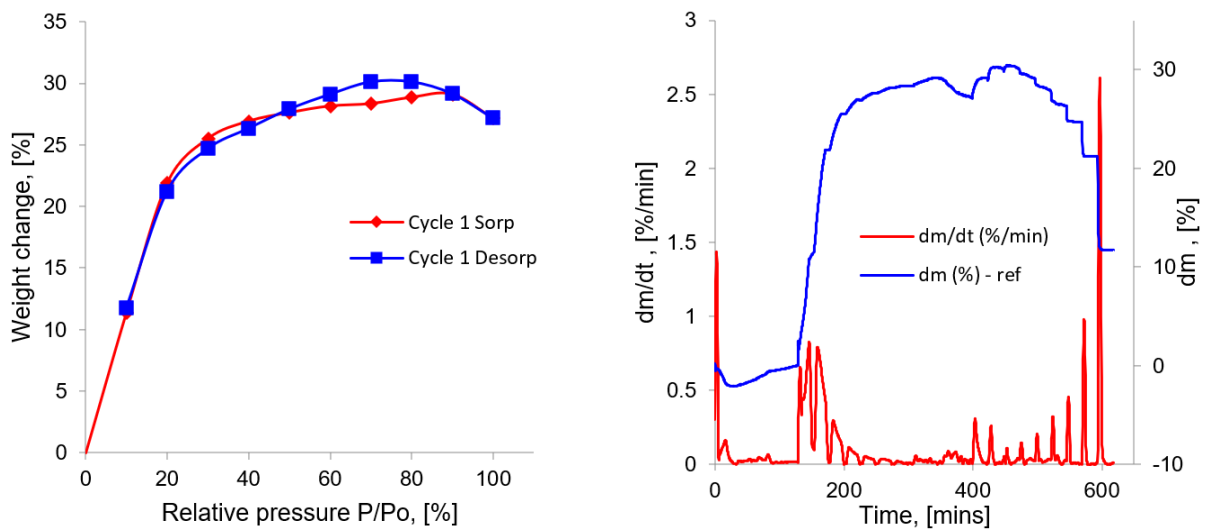


Figure 21 – Methanol adsorption on WA TONG at 60 °C. a) isotherm, b) kinetics

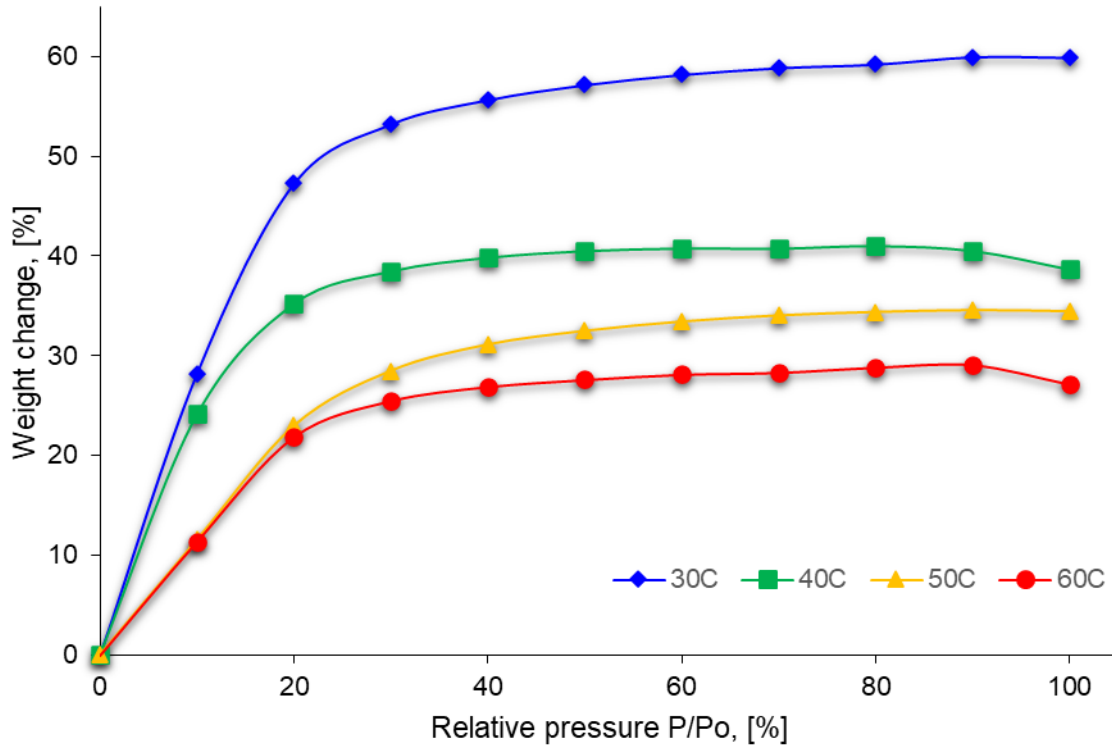


Figure 22 – An illustrative stack depiction of WA TONG sample adsorption isotherms at different temperatures

**Observation:** For sample WA TONG, the consistent trend from the above isotherm plots is that the sample exhibits isotherm of type I. its methanol adsorption uptake decreases with an increase of adsorption temperature. Hence the maximum uptake of about 60% adsorbent weight was on a 30 °C isotherm curve at saturation pressure condition. On isotherms at 40 and 60 °C, there's a deviation from the expected rising or plateauing isotherm curve trend around the saturation pressure zone. This led to what seems like a hysteresis between adsorption and desorption curves for which the plausible explanation is the insufficient equilibrium time. The sorption rate curve patterns on the respective kinetics matches the spotted deviations. Looking at the kinetics chart one can infer that with adjustment of adsorption step time (a bit larger timestep at the beginning of adsorption), the observed loop could have been mitigated and which would consequently lead higher adsorption uptake at even lower relative pressure.

## 5.1.2. Commercial samples – CWZ22P and CWZ22

### i. CWZ22P sample

At adsorption temperature 30 °C, reference sample weight – 22.29 mg, methanol saturation pressure at 30 °C - 21.83 kPa

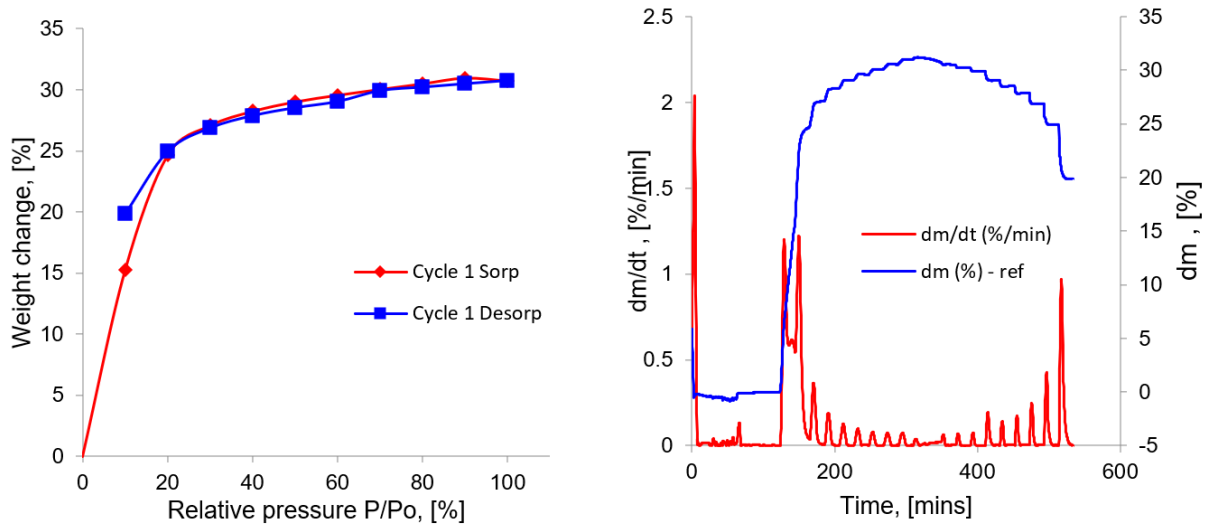


Figure 23 – Methanol adsorption on CWZ22P at 30 °C. a) isotherm, b) kinetics

At adsorption temperature 39.7 °C, reference sample weight – 22.34 mg, methanol saturation pressure at 40 °C - 35.38 kPa.

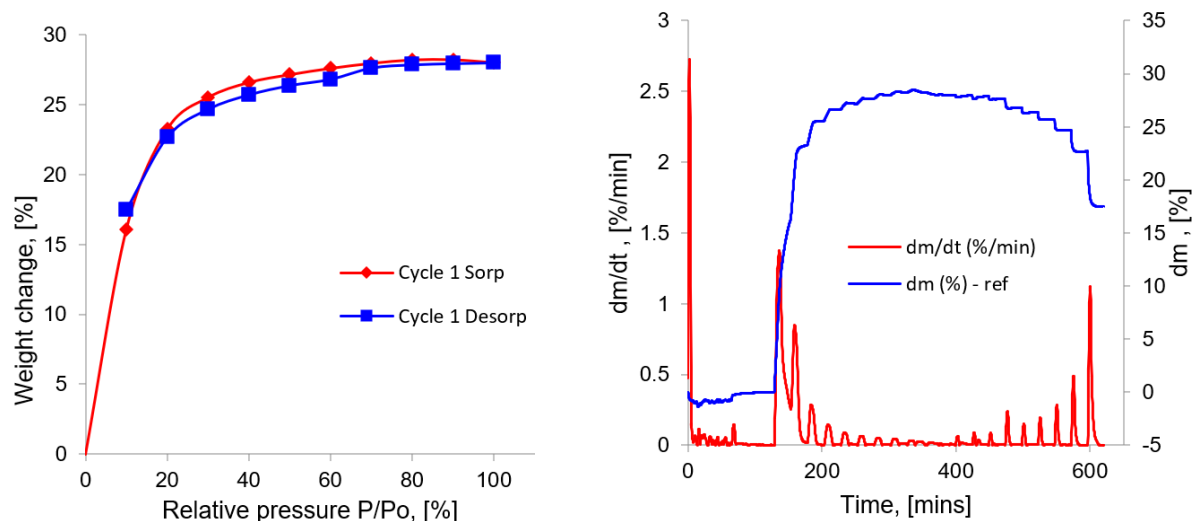


Figure 24 – Methanol adsorption on CWZ22P at 40 °C. a) isotherm, b) kinetics

At adsorption temperature 49.4 °C, reference sample weight – 22.29 mg, methanol saturation pressure at 50 °C – 55.47 kPa.



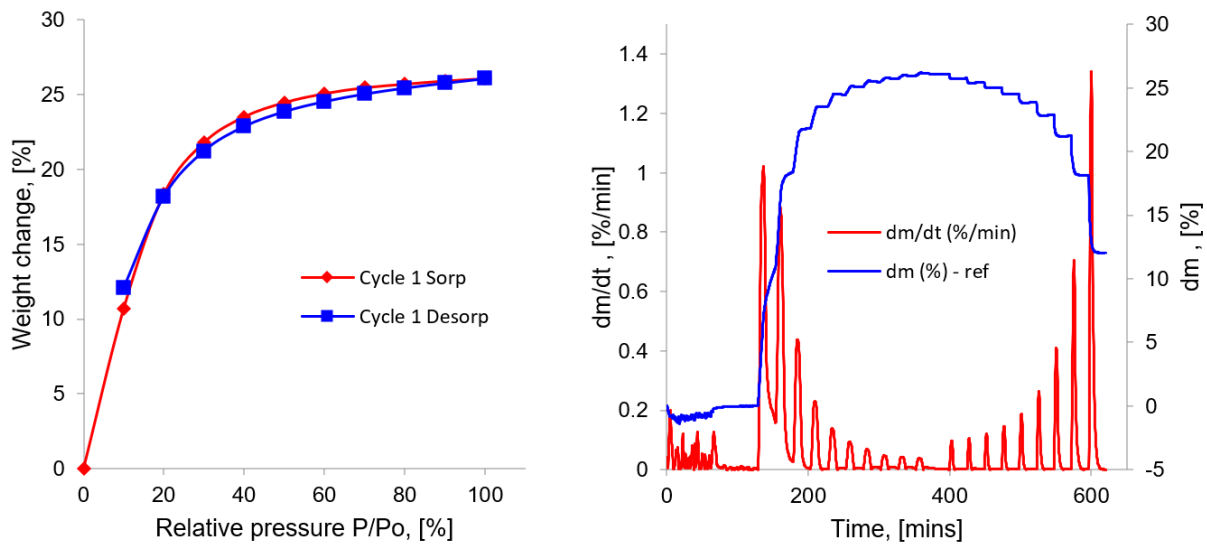


Figure 25 – Methanol adsorption on CWZ22P at 50 °C. a) isotherm, b) kinetics

At adsorption temperature 58.6 °C, reference sample weight – 22.25 mg, methanol saturation pressure at 60 °C – 84.40 kPa.

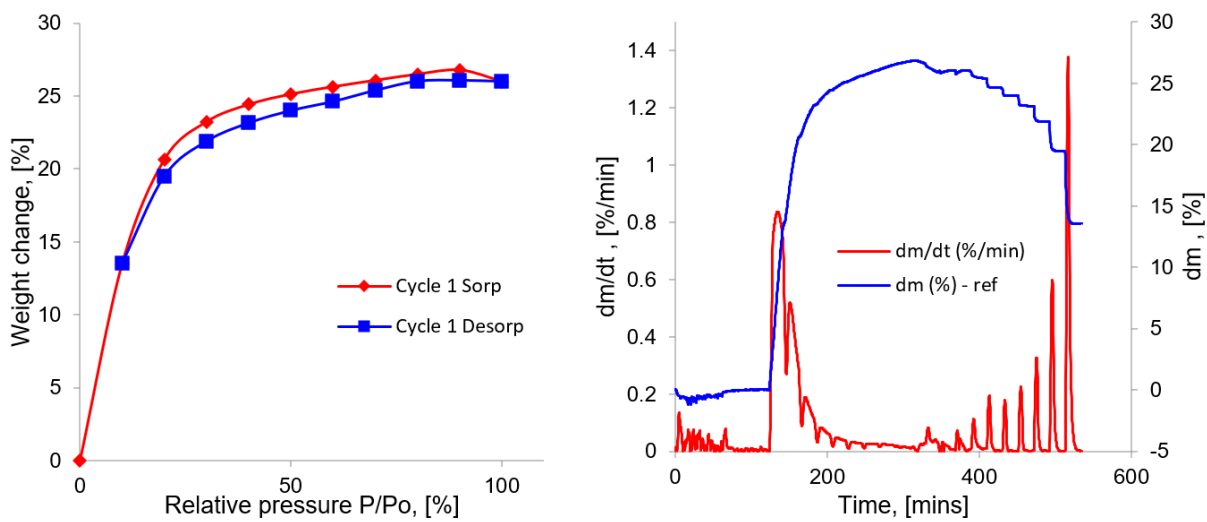


Figure 26 – Methanol adsorption on CWZ22P at 60 °C. a) isotherm, b) kinetics

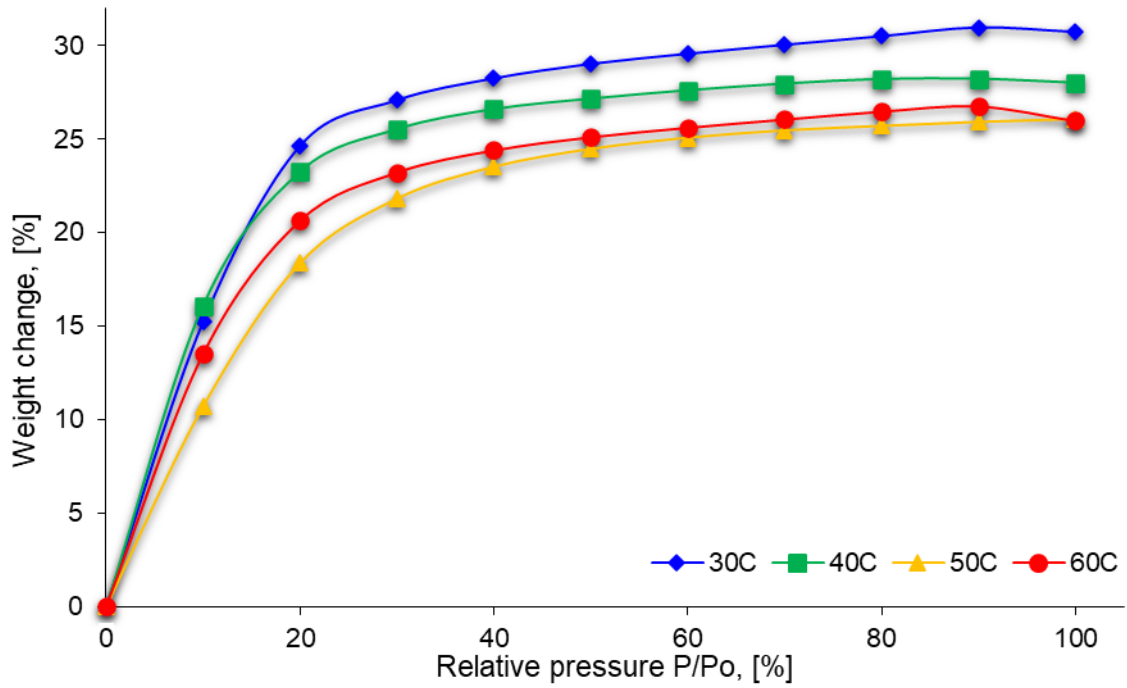


Figure 27 – An illustrative stack depiction of CWZ22P sample adsorption isotherms at different temperatures

**ii. CWZ22 sample**

At adsorption temperature 30 °C, reference sample weight – 18.76 mg, methanol saturation pressure at 30 °C – 21.83 kPa.

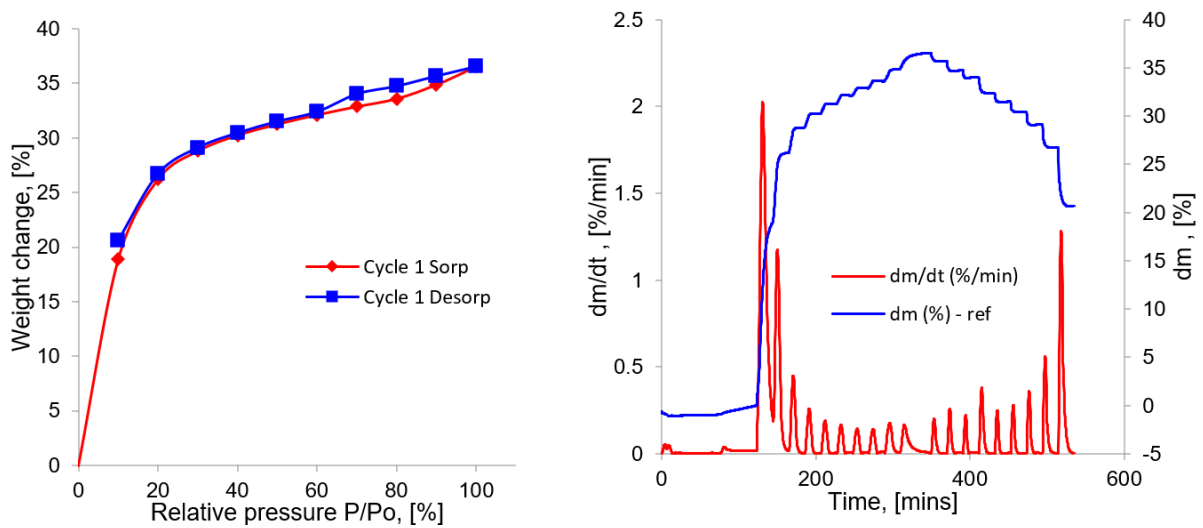


Figure 28 – Methanol adsorption on CWZ22 at 30 °C. a) isotherm, b) kinetics

At adsorption temperature 40 °C, reference sample weight – 19.17 mg, methanol saturation pressure at 40 °C - 35.38 kPa.

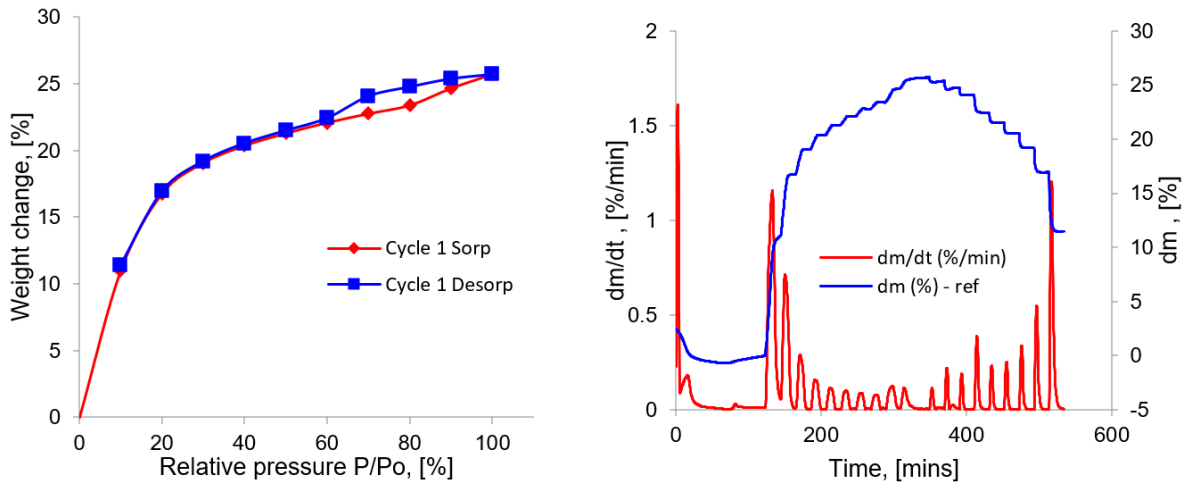


Figure 29 – Methanol adsorption on CWZ22 at 40 °C. a) isotherm, b) kinetics

At adsorption temperature 49.6 °C, reference sample weight – 18.73 mg, methanol saturation pressure at 50 °C – 55.47 kPa.

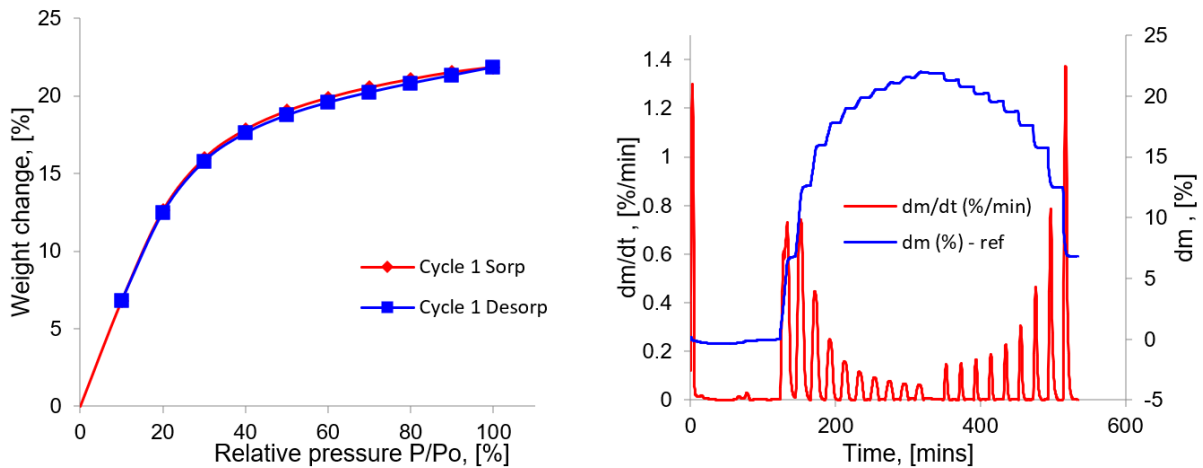


Figure 30 – Methanol adsorption on CWZ22 at 50 °C. a) isotherm, b) kinetics

At adsorption temperature 58.6 °C, reference sample weight – 20.41 mg, methanol saturation pressure at 60 °C – 84.40 kPa.

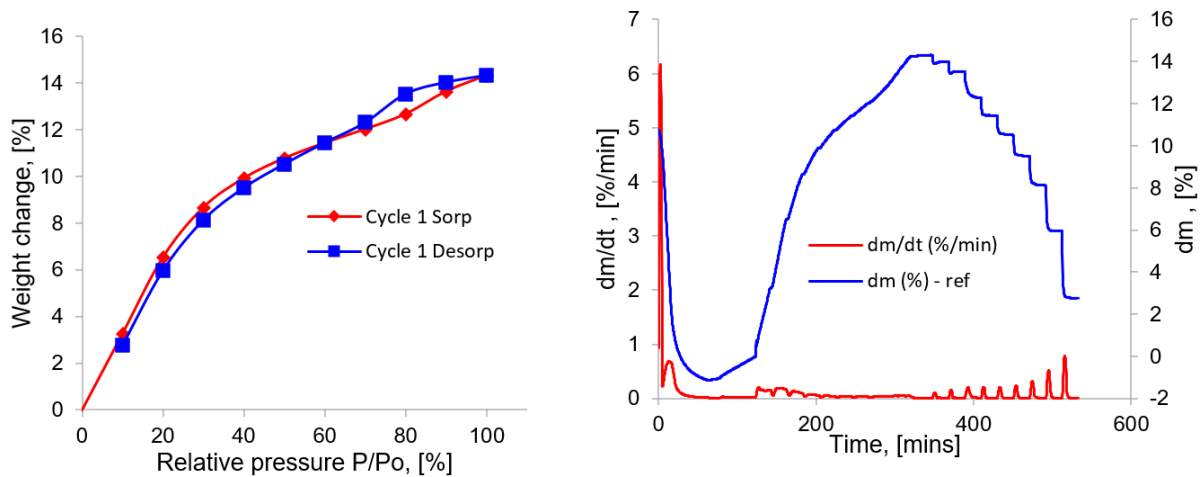


Figure 31 – Methanol adsorption on CWZ22 at 60 °C. a) isotherm, b) kinetics

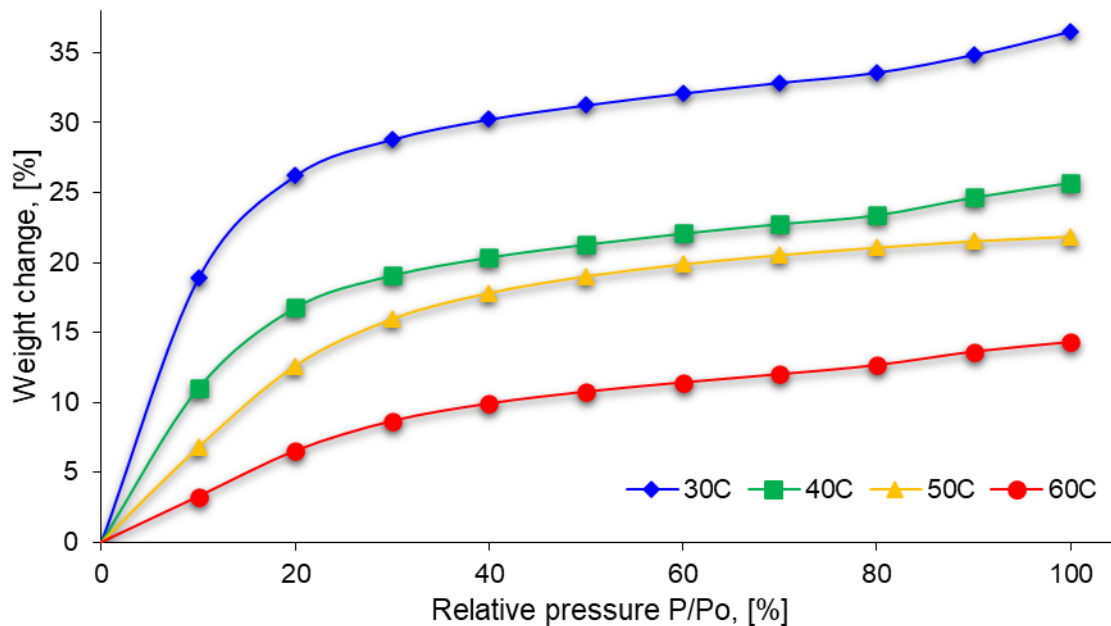


Figure 32 – An illustrative stack depiction of CWZ22 sample adsorption isotherms at different temperatures

**Observation:** Similar to sample WA TONG, both commercial samples CWZ22P and CWZ22 exhibits isotherm of type I. Methanol adsorption uptake decreases with an increase of adsorption temperature. The maximum methanol uptake for both samples was obtained at relative pressure of 1 on the 30 °C isotherm curve with approximate values of 27% and 36% adsorbent weight for CWZ22P and CWZ22, respectively.

## 5.2. Overall performance takeaways and comparison with in literature activated carbons

Like most activated carbon methanol pairs, all the three studied samples (WA TONG, CWZ22 and CWZ22P) resulted in adsorption isotherms of Type I which is indicative of strong adsorbate adsorbent interactions. The nature of these interactions depends on different parameters such as pore size distribution, surface complexes, the nature of the adsorbate, and isotherm temperature. In a predominantly microporous adsorbent adsorption happens mainly by pore filling mechanism [39]. At four adsorption temperature points of analysis, WA TONG - methanol isotherms exhibit characteristics typical for Type I Langmuir isotherm with subtle differences in the curve gradient rise to the plateau of the isotherm. For activated carbon samples the gradient rise is usually within the relative pressure ( $p/p_0$ ) range of 0.05-0.20 before reaching the inflection point [15]. The plausible explanation for these subtle deviations is the insufficient equilibrium time steps at respective points. Looking at the red adsorption rate curves on respective WA TONG kinetics charts at all four adsorption temperature points, there is inconsistency in peaks pattern relative to the predefined method timestep. The method timestep for all increments was set at 20 minutes. However, as the adsorption rate is usually higher at the start of the process, the fact that the adsorption curve fails to touch the base in the first three peaks shows the need to increase the step duration for the initial increments to ensure equilibrium is reached. This might have in turn improved the methanol adsorption uptake value at lower relative pressure.

Of the three studied samples, WA TONG exhibits superior sorption performance on all four adsorption temperature points of the analysis. Methanol adsorption uptake for WA TONG sample goes as high as 60 % of adsorbent weight on the 30 °C isotherm at a relative pressure of 0.9. The characterization analysis of WA TONG sample showed an average porosity and pore volume of about 61% and 0.73 cm<sup>3</sup>/g, respectively. This falls way below the in literature best performing methanol activated carbon adsorbent – Maxsorb III, whose methanol uptake at 30 °C adsorption temperature can reach up to 1.24 kg/kg (124%) at saturation conditions [31]. Maxsorb III is a highly microporous adsorbent with BET surface area of and micropore volume of about 3045 m<sup>2</sup>/g and 1.7 cm<sup>3</sup>/g, respectively [13].

However, in literature there are few activated samples with comparable adsorption uptakes to that of WA TONG at the working conditions similar to our experiment. In the study by Henninger et al where the methanol adsorption of six different activated carbons were put to test, sample Carbo Tech A35/1 exhibited an adsorption uptake of 0.58 kg/kg (58%) at the saturation conditions and adsorption temperature of 30 °C [32].

## 6. CONCLUSION

This thesis work involved a systematic study of a spruce based activated carbon sample WA TONG, its adsorption performance and potential applicability in adsorption chillers. The work highlighted the air conditioning challenge and the potential impact such niche of energy consumption poses to the environment. A brief review of the existing cooling solutions was presented with the emphasis on adsorption cooling technology. The description of preparation procedure of the activated carbon sample WA TONG, from the precursor material spruce lignin to the potassium hydroxide (KOH) activation of the hydrochar was outlined. Density, porosity and XRD characterization of the samples were done. The WA TONG samples exhibited similar crystalline structural pattern as the two commercial samples CWZ22PP and CWZ22, the sample was found to be predominantly amorphous in its carbonaceous nature.

Of the three studied samples, WA TONG presented superior adsorption performance at all four adsorption temperature points of the analysis. The maximum attained methanol uptake at saturation pressure conditions and adsorption temperature of 30 °C was found to be about 60% for WA TONG, 27% for CWZ22P and 36% for CWZ22. This fell short in comparison to the in literature best performing methanol activated carbon adsorbent – Maxsorb III whose adsorption capacity of 124% at similar working conditions. Subsequently this presents a technical limitation that could be a hindrance for adoption of such samples for commercial use adsorption chiller applications. There might exist a performance/cost tradeoff for biomass-based activated carbon adsorbents which could lead to wider adoption, hence further investigation study of the WA TONG sample on a pilot scale adsorption chiller could give more clarity on the subject.

### Future work to consider

- Further characterization of the samples like BET surface area, FTIR qualitative surface composition and SEM surface morphology analysis should be done for a better understanding of sample chemistry and adsorption mechanism.
- Further experimenting with the DVS method parameters to find a better fit equilibrium timestep could lead to higher adsorption uptake and also carrying out calculations of adsorption heat for studied activated carbon samples/methanol pair from the already obtained isotherms and kinetics results would lead to a more informed assessment of energy effectiveness the samples present.
- Changing the gravimetric ratio of KOH/Lignin char in the activation stage and also experimenting with alternative activating agents (H3P04 among others) could improve sample adsorption performance.

## Bibliography

- [1] The Future of Cooling. Opportunities for energy-efficient air conditioning. OECD/IEA 2018.
- [2] Ourworldindata. Energy mix – Is the world making progress in decarbonizing energy? <https://ourworldindata.org/energy-mix>. Source last checked on 06.05.2021.
- [3] BP Energy Outlook 2019, published in February 2019.
- [4] EIA International Energy Outlook 2019.
- [5] IEA, Shares of residential energy consumption by end use in selected IEA countries, 2017, IEA, Paris. IEA/shares of residential energy consumption by end use - 2017.
- [6] ARANER. Industrial Refrigeration - High-level information for developing the most efficient industrial refrigeration systems. 2019.
- [7] World bank – Four things you should know about sustainable cooling. <https://www.worldbank.org/Sustainable-cooling>. Source last checked on 06.05.2021
- [8] Minaal Sahlot, Saffa B. Riffat, Desiccant cooling systems: a review, International Journal of Low-Carbon Technologies, Volume 11, Issue 4, 15 December 2016, Pages 489–505
- [9] Ruzhu Wang, Liwei Wang and Jingyi Wu. Adsorption Refrigeration Technology Theory and Application. Shanghai Jiao Tong University, China. 2015
- [10] Anirban Sur, Randip K Das. Review on solar adsorption refrigeration cycle. International Journal of Mechanical Engineering & Technology (IJMET). 2010/7.
- [11] Mahmoud B. Elsheniti, Osama A. Elsamni, Raya K. Al-dadah, Saad Mahmoud, Eman Elsayed and Khaled Saleh. Adsorption Refrigeration Technologies. <http://dx.doi.org/10.5772/intechopen.73167>
- [12] Sur, Anirban & Das, Randip. (2016). Review of Technology Used to Improve Heat and Mass Transfer Characteristics of Adsorption Refrigeration System. International Journal of Air-Conditioning and Refrigeration. 24. <http://dx.doi.org/10.1142/S2010132516300032>
- [13] Faizan Shabir, Muhammad Sultan, Takahiko Miyazaki, Bidyut B. Saha, Ahmed Askalany, Imran Ali, Yuguang Zhou, Riaz Ahmad, Redmond R. Shamshiri. Recent updates on the adsorption capacities of adsorbent-adsorbate pairs for heat transformation applications. Renewable and Sustainable Energy Reviews. Volume 119, 2020, 109630, ISSN 1364-0321. <https://doi.org/10.1016/j.rser.2019.109630>
- [14] Mohammad A. Al-Ghouti, Dana A. Da'ana. Guidelines for the use and interpretation of adsorption isotherm models: A review. Journal of Hazardous Materials. Volume 393, 2020, 122383, ISSN 0304-3894. <https://doi.org/10.1016/j.jhazmat.2020.122383>
- [15] J. A. Menéndez-Díaz and I. Martín-Gullón. Types of carbon adsorbents and their production. Published in Activated carbon surfaces in environmental remediation (Interface science and technology series, 7) T. Bandosz Ed. ELSEVIER 2006 (ISBN: 0-12-370536-3) 1-48

- [16] Philippe Ouzilleau, Aïmen E. Gheribi, Patrice Chartrand, Gervais Soucy, Marc Monthieux. Why some carbons may or may not graphitize? The point of view of thermodynamics. *Carbon*. Volume 149. 2019. Pages 419-435. ISSN 0008-6223. <https://doi.org/10.1016/j.carbon.2019.04.018>
- [17] L.W Wang, J.Y Wu, R.Z Wang, Y.X Xu, S.G Wang, X.R Li. Study of the performance of activated carbon–methanol adsorption systems concerning heat and mass transfer. *Applied Thermal Engineering*. Volume 23, Issue 13. 2003. Pages 1605-1617. ISSN 1359-4311. [https://doi.org/10.1016/S1359-4311\(03\)00104-2](https://doi.org/10.1016/S1359-4311(03)00104-2)
- [18] Ng, K.C., Burhan, M., Shahzad, M.W. et al. A Universal Isotherm Model to Capture Adsorption Uptake and Energy Distribution of Porous Heterogeneous Surface. *Sci Rep* 7, 10634 (2017). <https://doi.org/10.1038/s41598-017-11156-6>
- [19] Heidarinejad, Z., Dehghani, M.H., Heidari, M. et al. Methods for preparation and activation of activated carbon: a review. *Environ Chem Lett* 18, 393–415 (2020). <https://doi.org/10.1007/s10311-019-00955-0>
- [20] Bronislaw Buczek, "Preparation of Active Carbon by Additional Activation with Potassium Hydroxide and Characterization of Their Properties", *Advances in Materials Science and Engineering*, vol. 2016, Article ID 5819208, 4 pages, 2016. <https://doi.org/10.1155/2016/5819208>
- [21] Hui TS, Zaini MAA (2015) Potassium hydroxide activation of activated carbon: a commentary. *Carbon Lett* 16:275–280. <https://doi.org/10.5714/CL.2015.16.4.275>
- [22] F. Derbyshire, M. Jagtoyen, R. Andrews, A. Rao, I. Martin-Gullón, and E. A. Grulke, "Carbon materials in environmental applications," *Chemistry and Physics of Carbon*, vol. 27, pp. 1–66, 2000. View at: [Google Scholar](#)
- [23] Yahya MA, Al-Qodah Z, Ngah CZ (2015) Agricultural bio-waste materials as potential sustainable precursors used for activated carbon production: a review. *Renew Sustain Energy Rev* 46:218–235. <https://doi.org/10.1016/j.rser.2015.02.051>
- [24] Abbadessa, A., Oinonen, P., and Henriksson, G. (2018). "Characterization of two novel bio-based materials from pulping Process side streams: Ecohelix and CleanFlow black lignin," *BioRes.* 13(4), 7606-7627. [https://bioresources.cnr.ncsu.edu/13\(4\)-7606-7627](https://bioresources.cnr.ncsu.edu/13(4)-7606-7627)
- [25] Wang, Kai & Vineyard, Edward. (2011). New Opportunities for Solar Adsorption Refrigeration. *Ashrae Journal*. 53. 14. [http://www.r744.com/files/1354\\_adref\\_Wang.pdf](http://www.r744.com/files/1354_adref_Wang.pdf)
- [26] Wang, R.Z. 2001. "Performance improvement of adsorption cooling by heat and mass recovery operation." *International Journal of Refrigeration* 24(7):602 – 611. [https://doi.org/10.1016/S0140-7007\(01\)00004-4](https://doi.org/10.1016/S0140-7007(01)00004-4)
- [27] Pons, M., F. Poyelle. 1999. "Adsorptive machines with advanced cycles for heat pumping or cooling applications." *International Journal of Refrigeration* 22(1):27 – 37. [https://doi.org/10.1016/S0140-7007\(97\)00042-X](https://doi.org/10.1016/S0140-7007(97)00042-X)



- [28] Kuchmacz J, Bieniek A, Mika Ł. The use of adsorption chillers for waste heat recovery. *Polityka Energetyczna – Energy Policy Journal*. 2019;22(2):89-106. <https://doi.org/10.33223/epj/108706>
- [29] Alghoul MA, Sulaiman MY, Azmi BZ, Wahab MAbd. Advances on multi-purpose solar adsorption systems for domestic refrigeration and water heating. 2007. *Applied Thermal Engineering* 27(5):813-822. <https://doi.org/10.1016/j.applthermaleng.2006.09.008>
- [30] D.C. Wang, Y.H. Li, D. Li, Y.Z. Xia, J.P. Zhang. A review on adsorption refrigeration technology and adsorption deterioration in physical adsorption systems. *Renewable and Sustainable Energy Reviews*. Volume 14, Issue 1. 2010. Pages 344-353. ISSN 1364-0321. <https://doi.org/10.1016/j.rser.2009.08.001>.
- [31] El-Sharkawy, M. Hassan, B.B. Saha, S. Koyama, M.M. Nasr. Study on adsorption of methanol onto carbon based adsorbents. *International Journal of Refrigeration*. Volume 32, Issue 7. 2009. Pages 1579-1586. ISSN 0140-7007. <https://doi.org/10.1016/j.ijrefrig.2009.06.011>.
- [32] S.K. Henninger, M. Schickanz, P.P.C. Hügenell, H. Sievers, H.-M. Henning. Evaluation of methanol adsorption on activated carbons for thermally driven chillers part I: Thermophysical characterization. *International Journal of Refrigeration*, Volume 35, Issue 3, 2012, Pages 543-553. ISSN 0140-7007. <https://doi.org/10.1016/j.ijrefrig.2011.10.004>.
- [33] NOAA National Centers for Environmental Information, State of the Climate: Global Climate Report for Annual 2020, published online January 2021, retrieved on April 29, 2021 from <https://www.ncdc.noaa.gov/sotc/global/202013>.
- [34] Zhigang Xie, Wei Guan, Fangying Ji, Zhongrong Song, Yanling Zhao. Production of Biologically Activated Carbon from Orange Peel and Landfill Leachate Subsequent Treatment Technology. *Journal of Chemistry*, vol. 2014, Article ID 491912, 9 pages, 2014. <https://doi.org/10.1155/2014/491912>
- [35] Das D, Samal DP, Meikap BC. Preparation of Activated Carbon from Green Coconut Shell and its Characterization. *J Chem Eng Process Technol*, 2015, 6: 248. <http://dx.doi.org/10.4172/2157-7048.1000248>
- [36] H Benaddi, T.J Bandosz, J Jagiello, J.A Schwarz, J.N Rouzaud, D Legras, F Béguin. Surface functionality and porosity of activated carbons obtained from chemical activation of wood. *Carbon*, Volume 38, Issue 5, 2000, Pages 669-674. ISSN 0008-6223. [https://doi.org/10.1016/S0008-6223\(99\)00134-7](https://doi.org/10.1016/S0008-6223(99)00134-7)
- [37] Linares-Solano A., Lozano-Castelló D., Lillo-Ródenas M.A., Cazorla-Amorós D. (2008) Controlling Porosity to Improve Activated Carbon Applications. In: Mota J.P., Lyubchik S. (eds) *Recent Advances in Adsorption Processes for Environmental Protection and Security*. NATO Science for Peace and Security Series C: Environmental Security. Springer, Dordrecht. [https://doi.org/10.1007/978-1-4020-6805-8\\_9](https://doi.org/10.1007/978-1-4020-6805-8_9)

- [38] Dynamic dual vapor gravimetric sorption analyzer - DVS Vacuum. Surface Measurement Systems. Apparatus instruction brochure. [surfacemeasurementsystems.com/DVS\\_Vacuum](http://surfacemeasurementsystems.com/DVS_Vacuum). Source last checked on 05.05.2021
- [39] Lodewyckx P. (2008) Adsorption on Activated Carbon: One Underlying Mechanism? In: Mota J.P., Lyubchik S. (eds) Recent Advances in Adsorption Processes for Environmental Protection and Security. NATO Science for Peace and Security Series C: Environmental Security. Springer, Dordrecht. [https://doi.org/10.1007/978-1-4020-6805-8\\_3](https://doi.org/10.1007/978-1-4020-6805-8_3)

